

Project name:

**Integration and exploitation of networked Solar radiation Databases for environment monitoring**

Project acronym:

**SoDa**

Contract number:

**IST-1999-12245**

Deliverable title:

**Joint Report on Interpolation Scheme "Meteosat" and Database "Climatology I (Meteosat)"**

Deliverable number:

**D 3-8 and D5-1-4**

Type of deliverable:

**Report**

Security:

Author:

**ENSMP (M. Lefèvre, M. Albuissou, L. Wald)**

Contributors:

Contractual date of delivery to the Commission:

**December 2001 and June 2002**

Actual date of delivery to the Commission:

**June 2002**

## Abstract

The joint deliverable D3-8 and D5-1-4 describes the implementation of the method Heliosat-II (D5-1-4), the construction of the database (D3-8) and the resource permitting to exploit the database through the SoDa IS.

The method Heliosat-II was developed in the WP 3.4 in 2000-2001. It converts images acquired by the satellite Meteosat into maps of global irradiation received at ground level. The object of the WP 5.1d is the implementation of this method for its application to Meteosat archives, and using the resources in the SoDa service, in order to create time-series of daily irradiation for Africa, Europe, and the Atlantic Ocean. In WP 3.5c, the WP 5.1d application is applied to a time-series of Meteosat images spanning from 1985 onwards. A database is created that serves irradiation information that supports the resource WP 5.3r "Meteosat" delivering irradiation values through the SoDa IS. The resource WP 5.3r will serve the resources devoted to vegetation, climate studies and ocean applications as well as to solar systems, among others. In the course of the work, an extension of the resource permitted to perform the resource WP 5.3f as well.

The report discusses the users requirements, their satisfaction and the specifications of the resource and of the database. It presents the database properties and the operational implementation of the method Heliosat-II. Finally, it details the service execution. All equations and practical details of the application WP 5.1d are given in Annexes.

The present document reports on these four different and related activities: WP 5.1d, WP 3.5c, WP 5.3f and 5.3r. Changes in the schedule and work programme performed under the supervision of the scientific co-ordinator permitted to run these activities partly in a concurrent way. They are completed in the same period and the delay that was foreseen in January 2002 for WP 3.5c was partly mitigated.

The method Heliosat-II was successfully implemented. Coincident ground measurements were used for checking that the application reproduces the measurements with the accuracy defined in WP 3.4. The method Heliosat-II itself is not a resource of the SoDa service; its execution calls upon SoDa resources and other outcomes, namely, the method resulting from WP 3.4, including the calibration of Meteosat images, the modelling of the irradiation under clear skies (WP 5.2), the screening for quality-check (WP 3.5c), the Linke turbidity factor (WP 5.2a), the interpolation method (WP 5.1a) and the orography (WP 5.3o).

This final database of WP 3.5c is a medium-resolution climatological database of 3-hour irradiation for Africa, Europe, and the Atlantic Ocean. Comparisons were made between the outputs of this database (daily irradiation, monthly means of daily irradiation, 5-days and 10-days irradiation) and the ground-based measurements for Europe and Africa and for several years. The accuracies are compliant with the specifications. This demonstrates both the quality of the method Heliosat-II and the correct implementation of the application.

The database comprises the equivalent of 118500 stations. When compared to the stations that are available through the WMO network, the database offers a much more detailed knowledge of the spatial distribution of the solar radiation, two orders of magnitude larger than the present knowledge.

## Table of Contents

Abstract.....	2
Introduction.....	4
User Requirements, their Satisfaction and Specifications .....	5
The Data Model, Database and Storage Constraints.....	8
Operational Implementation of the Method Heliosat-II .....	10
Service Execution .....	12
References.....	15
Annex A. Notations .....	21
Astronomical quantities and sun angles.....	21
Radiation quantities .....	21
Notations for describing the optical properties of the atmosphere and the ground .....	22
Notations for other properties of the site .....	23
Satellite (Meteosat) -related quantities .....	23
Annex B. Overview of the method Heliosat-II.....	24
Annex C. Modelling the global, direct and diffuse irradiances under clear-skies .....	25
The beam component.....	26
The diffuse component .....	27
The global irradiation.....	28
Annex D. The cloud index.....	29
Annex E. The computation of the ground albedo.....	31
Annex F. The computation of the cloud albedo.....	32
Annex G. The relationship between the cloud index and the global hourly irradiation .....	33
Annex H. The computation of the daily irradiation and subsequent quantities .....	34
Annex I. Solving the specific case of sun glitter on the ocean .....	35
Annex J. An additional correction to hourly irradiation estimates .....	37

## Introduction

The joint deliverable D3-8 and D5-1-4 describes the implementation of the method Heliosat-II (D5-1-4), the construction of the database (D3-8) and the resource permitting to exploit the database through the SoDa IS.

The method Heliosat-II was developed in the WP 3.4 in 2000-2001 and was reported in the deliverable D3-2. The method Heliosat-II converts images acquired by the satellite Meteosat into maps of global irradiation received at ground level. It was proved that the method Heliosat-II provides better results than its state-of-the-art counterparts do. The accuracy was assessed by the means of a comparison with measurements made in the meteorological network in Europe.

The object of the WP 5.1d is the implementation of the method Heliosat-II for its application to Meteosat archives, and using the resources in the SoDa service, in order to create time-series of daily irradiation for Africa, Europe, and the Atlantic Ocean. Four months of coincident ground measurements and Meteosat data are used for testing the correct implementation. It was checked that the application reproduces the measurements with the accuracy defined in WP 3.4, using different measurements than those used to test the development of the method Heliosat-II. The consistency with the products, created in WPs 3.5a and b, on the overlapping zone was also checked. The application was found compliant to the specifications and it was decided to proceed with it. Though the method Heliosat-II itself is not a resource of the SoDa service, its execution calls upon SoDa resources and other outcomes, namely, the method resulting from WP 3.4, including the calibration of the Meteosat images, the modelling of the irradiation under clear skies (WP 5.2), the screening for quality-check (WP 3.5c), the Linke turbidity factor (WP 5.2a), the interpolation method (WP 5.1a) and the orography (WP 5.3o).

In WP 3.5c, the WP 5.1d application is applied to a time-series of Meteosat images spanning from 1985 onwards. To date, the time-series is made of two sets of 40908 images each, one set in the visible range, the other in the thermal infrared range. This database of images was established by the means of the Minimage software, freely available by the Ecole des Mines de Paris. The two datasets are separate and each Meteosat image is a layer within an image Minimage framework, one framework per day. This differs from the original Open MTP formats of the provider Eumetsat. This format was selected a more suitable for the further processing and because the Open MTP formats evolved in time. This database is intended only for a private access by the application Heliosat-II. Accordingly, it was organised in directories and sub-directories tailored to this application. Each image was quality-checked on receipt using a semi-automatic visual screening. Though the work to create this database was considerable, this database of images should only be considered as an intermediate database.

Another "intermediate" database was created in this WP 3.5c, composed of measurements of hourly and daily irradiances made in the world meteorological network (World Wide Watch). Hourly data were collected for Europe from the national weather services and span from July 1994 to June 1995 for 60 sites. A special effort was made in co-ordination with Ecole Nationale d'Ingénieurs in Bamako (Mali) to collect observations over Africa, a continent where few measurements are available. It resulted into the collection of measurements of daily irradiation spanning over at least one year for 30 sites. Half of them have data for periods of 4 years or larger. The original datasets were harmonised for formats, units and time system. The UTC time system was selected as it is that ruling Earth observation missions and adopted for the final database in WP 3.5c. The measurements were quality-checked. This activity led to the development of a web service allowing customers to control the quality of their own time-series of measurements. This service is presently available in the server [www.helioclim.net](http://www.helioclim.net) and is a clear contribution to standardisation issues. An article was submitted to the international journal *Solar Energy* (see Annex C of the QMR 8). The data were used by the partner

Meteotest for assessing the Linke turbidity factor (WP 5.2a) and were used in WP 3.5c for checking the quality of the products resulting from the final database.

This final database of WP 3.5c is a medium-resolution climatological database of 3-hour irradiation for Africa, Europe, and the Atlantic Ocean, spanning from 1985 onwards. This database is detailed in this report. Comparisons were made between the outputs of this database (daily irradiation, monthly means of daily irradiation, 5-days and 10-days irradiation) and the ground-based measurements for Europe and Africa and for several years. The accuracies are compliant with the specifications. This demonstrates both the quality of the method Heliosat-II and the correct implementation of the application.

The database of WP 3.5c supports the resource WP 5.3r "Meteosat" delivering irradiation values through the SoDa IS. The specifications of the resource are given in this report. The resource WP 5.3r will serve the resources devoted to vegetation, climate studies and ocean applications as well as to solar systems, among others. In the initial plan, the resource WP 5.3f was to be developed to offer an access to daily irradiation from the database "high resolution solar radiation database" (WP 3.5b). The purpose of this database is to support the computation of detailed statistics of half-hourly irradiation in a limited period (5 years). Its design was made in this respect and random access to specific periods for the computation of daily irradiation from half-hourly values of cloud index is not easy and not fast. Since the WP 3.2 demonstrated the consistency of the resulting products with those that can be computed from the high resolution database, the service for daily irradiation can be best offered by the resource WP 5.3r and both resources are merged.

The present document reports on these three different and related activities: WP 5.1d, WP 3.5c, WP 5.3f and WP 5.3r. Changes in the schedule and work programme performed under the supervision of the scientific co-ordinator permitted to run these activities partly in a concurrent way. They are completed in the same period and that the delay that was foreseen in January 2002 for WP 3.5c was partly mitigated.

The initial schedule planned a completion of WP 5.1d in December 2001, of WP 3.5c in May 2002, of WP 5.3f in July 2002 and of WP 5.3r in June 2002 (Technical Annex to the contract, detailed in Action Plan). The revised schedule made in January 2002 has foreseen a completion of WP 5.1d in April 2002 because of delays in WP 5.1a "Turbidity" (deliverable D5-2-1) and consequently, a completion of WP 3.5c in September 2002. By making different persons working on complementary aspects, time was gained. The WP 5.1d was completed in April 2002, the WP 5.3f, r were completed in June 2002 and the WP 3.5c was completed in July 2002. The database comprises 13 years of data. The final delay for the whole operation is therefore 1 month. The updating of the database is on-going and is performed by ENSMP.

The report discusses the users requirements, their satisfaction and the specifications of the resource and of the database. It presents the database properties and the operational implementation of the method Heliosat-II. Finally, it details the service execution. All equations and practical details of the application WP 5.1d are given in Annexes.

### User Requirements, their Satisfaction and Specifications

The design of the resource takes into account the user requirements (deliverable D6-1) and the results of the series of tests of the first prototype of the SoDa service (deliverable D6-2). The design, GUI and other aspects of other Web services were also taken into account: INFEO, EEA-EIONET, CERES, EO Newsroom, IFREMER-SISMER, MODB, MedAtlas, NASA, NOAA-NCDC, USGS, Unidata, RETScreen, HelioClim, SWITCH, Environment Canada, Satel-Light, SWERA, NREL, DLR, IPCC, WMO, WMO-World Radiation Data Center. CD products were also analysed: CERES, EUMETNET-

European Climate Data Set, WMO-CLINO, Meteonorm, ESRA, ISCCP, ISLCP, Global-Land 1-km AVHRR, Medias-France, Global Daily Summary, Global Upper Air Climatic Atlas, Meteosat Collection, Earth observation by Meteosat, NASA-SAGE, NASA-SRB, IPCC Data Distribution Centre, ISLCP.

Demands from users consist in time-series of global hourly and daily irradiation and derived quantities (e.g., 5-days sums and 10-days sums for agricultural or health applications). Time-series should be long enough, at least one year but longer periods are highly preferable. Geographical coverage is preferably the whole world. Though this quantity is not well expressed because of its complexity, the requested size of the spatial support is of order of 10 km, that is 5' of arc angle. There are some demands for higher spatial resolution, 1 km.

The requirements for accuracy depend upon the requested parameter and are listed in the Table below, expressed as RMSE (root mean square error).

Type	Irradiation ( $Wh\ m^{-2}$ )	Type	Irradiance ( $W\ m^{-2}$ )
Hourly values	130	Hour	130
Daily values	800	Day	35
5-days sum of daily irradiation	3000	5-days	25
10-days sum of daily irradiation	5500	10-days	20
Monthly mean of hourly irradiation	80	Month	15
Monthly mean of daily irradiation	400		

Table 1. Requirements for accuracy expressed as RMSE for irradiation ( $Wh\ m^{-2}$ ) and irradiance ( $W\ m^{-2}$ )

Several publications demonstrate that these requirements can only be met by an appropriate processing of images taken by the meteorological geostationary satellites. The deliverable D3-2 demonstrate that the method Heliosat-II provide results whose accuracy is compatible with the requirements in Table 1.

A major problem arises to satisfy the space and time requirements. Satellite data are not given free and the purchase of several years of satellite images may reveal very expensive. For example, NASA requested approximately 20 kEuro for one year of data for each of the satellite GOES-E and -W. In other places: China (FY-2), India (INSAT), Japan (GMS) and Russia (GOMS), we attempted to contact appropriate persons within the responsible national agencies to discuss the collection of data. They reveal unfruitful. Negotiations with Eumetsat were most satisfactory. Given a small fee, Eumetsat agreed to provide Meteosat images of reduced resolution covering one-third of the Earth. Centred on the Gulf of Guinea, these images cover Europe and Africa, which are the areas most demanded by the customers of the SoDa service (Fig. 1). The time-series secured by Armines/ENSMP starts from the creation of this set, in 1985. In this time-series, images are available only every 3 hours, following the standards of the World Weather Watch. Because interpolation in time is not reliable in this case, we decided to restrict the service to the delivery of daily values and not to provide hourly values. However, in order to keep this option open, we decided to store these hourly values in the database. It will be easy then to deliver them if decision is taken. It should be added that algorithmic tools exist that create synthetic hourly irradiation values given a daily irradiation. The prototype of the SoDa service comprises such resources that can be piped with the present resource via the SoDa Compound Service.

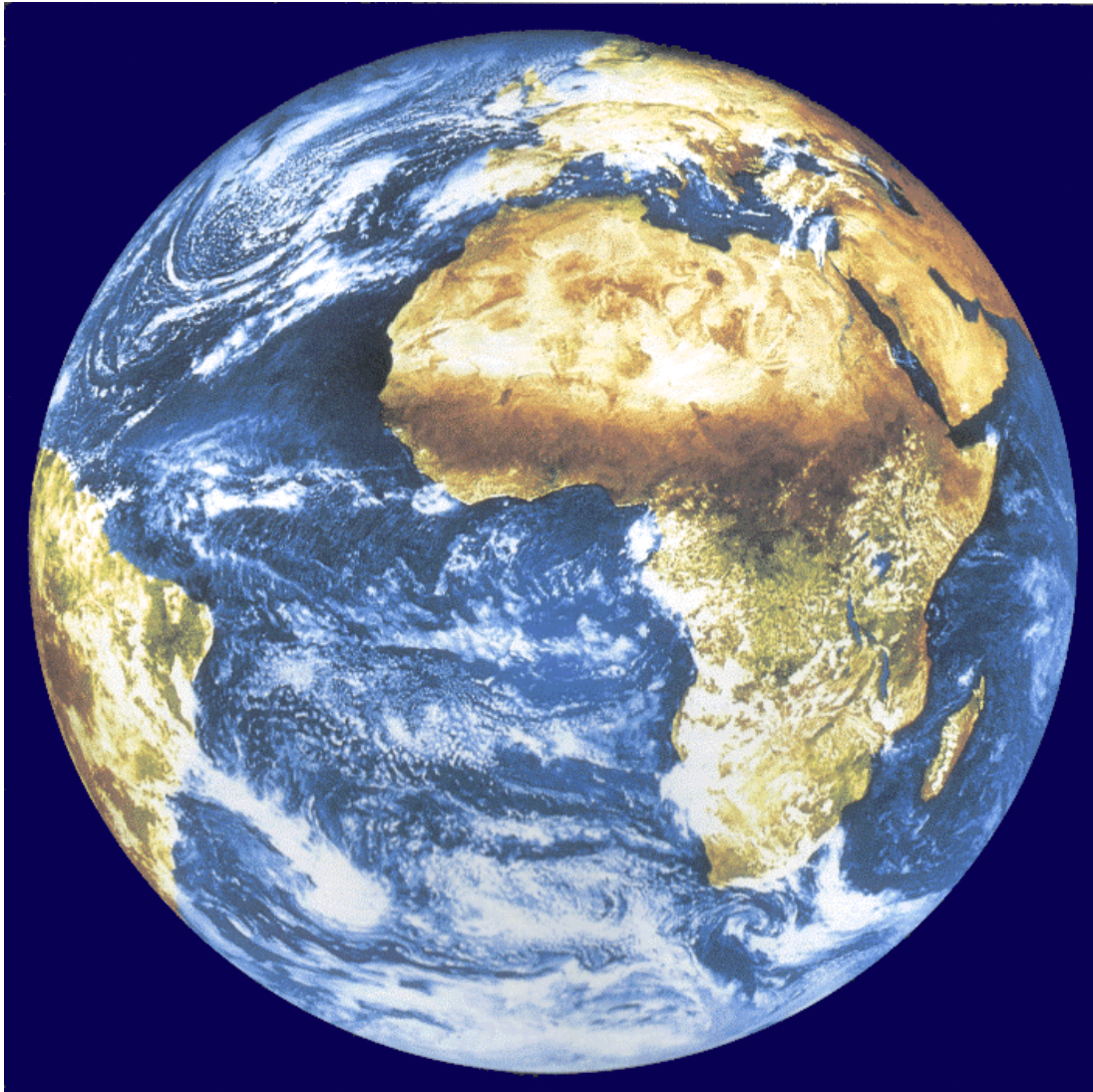


*Figure 1. A Meteosat image*

Though the size of the spatial support of these B2 images is compatible with the requirements, their particular mode of production means that a pixel of say, 10 km in size, is available every 60 km in both directions. It follows that the resource will call upon the interpolation procedure defined in deliverable D5-1-1. The study of the method Heliosat-II (deliverable D3-2) performed comparisons with WMO data and showed the compliance in accuracy of the interpolated values.

Parameters should be irradiation in  $\text{Wh m}^{-2}$  or irradiance in  $\text{W m}^{-2}$ . It may be possible to offer a change in units, especially for irradiation. In meteorology and agriculture, one uses  $\text{J cm}^{-2}$ , persons working in the field of solar energy:  $\text{Wh m}^{-2}$  and others Ly (Langley). Since the outputs originate from an integration of data held in the database, a parameter should be provided denoting the reliability of the estimate.

Another parameter was requested by two customers working in oceanography and whose interest lies in the assessment of the sea surface temperature using thermal infrared sensors aboard polar orbiting satellites such as the NOAA-AVHRR, ESA-ERS-ATSR, ESA-Envisat-AATSR. The atmospheric transmittance should be modelled and they believed that an estimate of the transmittance in the sun

broadband range may help in better assess the transmittance in the thermal range. The broadband transmittance is what is termed clearness index in solar energy.

Requirements about geographical and temporal selection are those already in use in the SoDa IS GUI (tags <geopoint> and <timeperiod> of the SoDa XML).

Except for hourly values, requirements are based upon the time unit "day". To keep the service open to further requests from customers, e.g. two-week sums of irradiation, we decided to store only daily values. The construction of the final quantities will be done through the additional functions. The attributes of <timeperiod> are set accordingly.

The geographical system used by <geopoint> is the same than that used by EUMETSAT and weather services. No change is requested.

Customers request a near real time answer. The retrieval of the data should be fast as well as the on-line processing. An important aspect of the requirements is that the large majority of customers requested time-series for a specific location and not time-series of gridded (maps) values. We decided to discard the image structure and to shape the database to facilitate the search for time-series for a given location. The requested location is usually not a B2-pixel. It follows that answering a request needs the extraction of time-series of the four neighbourhood B2-pixels and the interpolation of each daily value. Accordingly, additional functions should be added between the extraction functions and the request functions. For speed reasons, the interpolation procedure will be embedded in these additional functions instead of calling it within the Soda Compound Service.

Customers are accessing the Soda service via standard browser. The size of the XML outputs of the resource should not be too large. In view of the experience of other resources and other services, a trade-off between the speed of answer, the bandwidth, user requirements and user-friendly aspects of the GUI is established as one year of daily values.

The execution of the service requests access to resources of the SoDa service. The execution of the method Heliosat-II requests information from the SoDa service. Since the method Heliosat-II itself is not a resource, and since speed is at stake, the data (orography, Linke turbidity factor, Meteosat calibration coefficients) necessary for the execution of the method Heliosat-II are obtained through prior HTTP Get to the corresponding URLs in system calls in the C software. It would have been possible to make software using the Compound Service at the expenses of computational resources and time.

### The Data Model, Database and Storage Constraints

The data model follows that of the WMO / WCP with a few exceptions. Data are defined in time and space and has defined units (SI). Our data model is compliant with that of WMO as for the provider, units, time period, time sampling, time support, geographical location.

For the time sampling in the database, we are not using exactly the time system (UTC) of WMO, but that of Eumetsat, the European federation of Met-Offices, for the satellite data. The time is expressed in half-hour in UTC, noted slot, ranging from 1 to 48. The time support is still the hour. This Eumetsat / MOP time system will change as we evolve towards the next generation of satellite products MSG. However, as the time sampling of the sensor is kept as additional information, knowing the geographical location is the site permits an accurate conversion from one system to the other. They should be considered as equivalent. It should be mentioned that the time system used for the exploitation application is UTC.

Following the WMO/WCP model, each data is stored as a couple of (time, value). Use of the Eumetsat time system and additional parameters permits to store time on a byte only. Deviation is made from the WMO/WCP model by not storing explicitly the day (number or date). The day is retrieved by the biunivocal relationship between the day and the address of the series of values for this day in the database, knowing that there are eight couples per day.

The WMO/WCP model is not dealing with gridded data and thus does not comprise attributes on space support and sampling. By assuming that the support of the information, approximately 100 km<sup>2</sup>, can be assimilated to a time-averaged pin-point measurements, as demonstrated in the literature (see also discussion in deliverable D3-2), we assimilate the Meteosat-derived measurements to WMO measurements and it is not necessary to add components to the WMO/WCP model. This is additionally substantiated by the fact that the geographical location of the WMO measuring stations are given with an accuracy of 1' of arc angle, which is fairly close to the 5' of the support of our estimates.

The WMO/WCP model comprises a description of the measuring station with several attributes, such as latitude, longitude, elevation above sea level, name, country and a digital identifier. The attributes "name" and "country" are not kept since they have no signification in our case. We defined an identifier in our own nomenclature as follows. Scanning the Meteosat image of 416 times 416 pixels, starting from the upper leftmost corner, we reject pixels that are outside the Earth disk as seen by Meteosat and the pixels for which the elevation angle under which Meteosat is seen from this location, is smaller than 15° - the physical model being not accurate for such angles. The remaining pixels are labelled by their ranking order; this ranking order is the identifier.

The database comprises the equivalent of 118500 stations. This number may be compared to the 70 sites offering daily values for a period of similar duration that are available for Europe in the ESRA (2000) and the 30 stations in Africa with daily values for more than four years available through the WMO World Radiation Data Center. The database offers a much more detailed knowledge of the spatial distribution of the solar radiation, two orders of magnitude larger than the present knowledge.

A table is set that offers a correspondence between the identifier, the location of the pixel in lines and rows and the geographical location in latitude and longitude. In order to gain storage space, we opted for less redundancy than the WMO/WCP model. Instead of repeating all attributes for each time-series for a station, we repeated only the identifier. This table is in binary format.

As for the database, we opted for a binary proprietary format because the data model is very simple, only one parameter is stored and the overall structure is simple. Unless the usage in weather data where there is one file per station and per year, we made a unique file for all pixels for one year. Though it is an unstructured binary file, one may describe it approximately as a set of records, one record per station with a fixed length. A record begins with the identifier, followed by 366 sets of eight couples of time and value. One file contains approximately 1 Giga-values. This choice of the structure permits also to speed up the access to data.

Given the speed of the exploitation software, the storage constraints were given a high priority. Compressed format was rejected because of access time. This also explains the choice of binary format. Storing hourly irradiation requests two bytes, except if one uses different units, resulting also in a loss of accuracy. Storing daily irradiation also requests two bytes. Storing sums over 5 days or 10 days or a month requests more than two bytes. We opted for not storing derived quantities, such as daily values, or 5-day and 10-day sums, or monthly sums or monthly means. These quantities will be computed on the fly by the application.

A further gain is made by storing the cloud index, a quantity ranging between -0.2 and 1.1, as a byte after an appropriate offset and multiplication. This choice is also that made by the WP 3.5b. When the

cloud index value is unknown (e.g., lack of original data, unreliable estimate), the cloud index is set to 255. Finally, the size of a yearly file is approximately 1 GByte.

An additional table is created in order to increase computing speed of the exploitation software by reducing access to the SoDa resources. For each identifier (each pixel), a series of calls were made to the appropriate SoDa resources to get the monthly values of the Linke turbidity factor and the altitude of the pixel. These values are stored in the table. They are used by the WP 5.1d application (heliosat), producing the cloud index from the Meteosat images, and by the exploitation software (helio\_gd).

Figure 2 depicts the construction of the database of quality-checked Meteosat images on which the method Heliosat-II is performed.

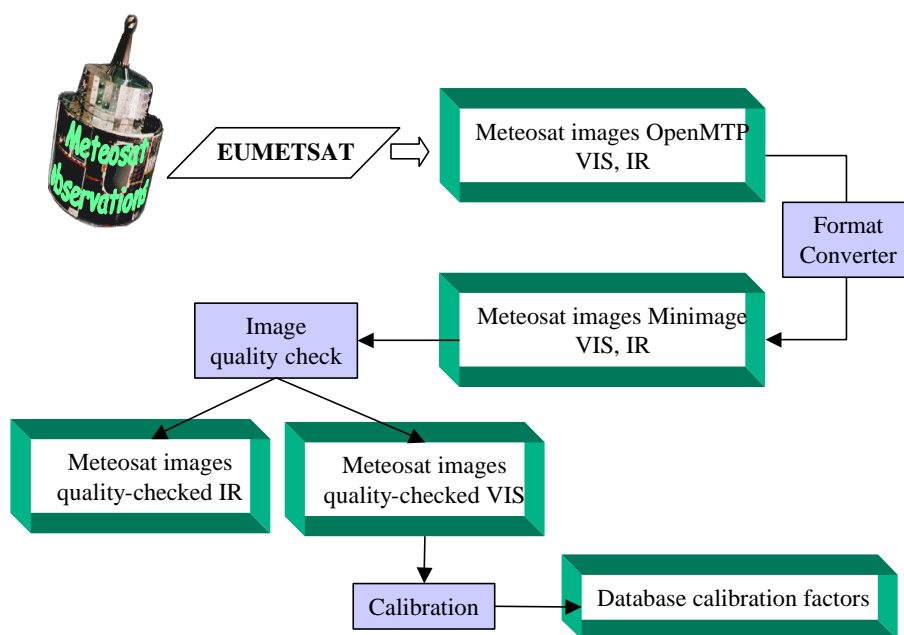


Figure 2. Construction of quality-checked Meteosat images database and of the calibration factors database

### Operational Implementation of the Method Heliosat-II

Given the choice made for the database, the method Heliosat-II is implemented in two separate components: heliosat and helio\_gd. The first one processes the series of Meteosat images, computes cloud indices and stores them into the database. The second one exploits the database and converts cloud indices into appropriate variables: daily irradiation, 5-day irradiation etc.

Both softwares are written in C, using the software Minimage. Constraint on time execution is important though non critical. In that respect, some data (orography, Linke turbidity factor) necessary for the execution of the method Heliosat-II were obtained from the Soda service once for all and stored in the database. Other data that depend upon the day and the geographical location of the site requested by the customer (orography, Meteosat calibration coefficients) are obtained through HTTP Get to the corresponding URLs in system calls in the C software. It would have been possible to make software using the Compound Service at the expenses of computational resources and time.

The software heliosat is entirely automatic; it performs on a series of images contained in a given directory. The image files were named in such a way that the name contains all information that is necessary for the processing, namely instant of acquisition by the sensor. It makes use of the two tables of the database. For each image, there is a request to the database of the calibration coefficients through a HTTP Get call to the server *www.helioclim.org*. Of course, the automatic application of the method Heliosat-II to several years of images necessitated some adaptations. Two additional developments were made. One deals with the method for creating the maps of ground albedo, and especially the problem of the initial state in an iterative procedure. The second treats the case of the oceanic areas affected by the sun glitter effects that may falsely result in very low irradiation. Statistics are locally computed on the image to correct these effects. The Annexes detail the algorithms used in the softwares heliosat and helio\_gd.

The software heliosat runs on a Unix machine and processes one year of data in 3 days (execution time) in a completely automatic way. Meteosat images are presently stored on Exabytes and are downloaded year after year. Then heliosat is run. The database is increased. The Meteosat images are erased from the disk and another year is downloaded on the disk. A scheme of this execution is shown in Figure 3.

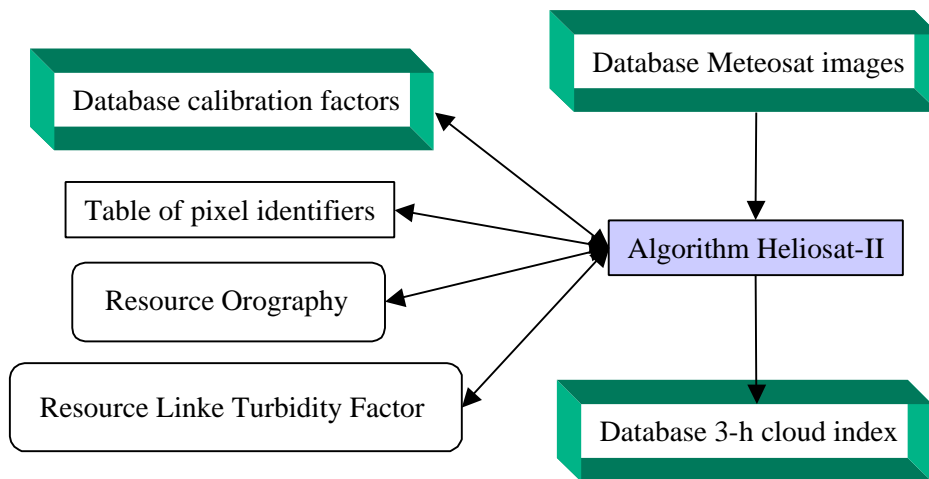


Figure 3

The software helio\_gd reads the database and converts the cloud index into hourly clearness index for each of the days of the requested period. The hourly clearness indices are then converted into daily irradiation or in irradiance for this day (see Annexes). The necessary information on the Linke turbidity factor and pixel elevation is found in the database. The time-series of daily irradiation is then converted into the requested variable: daily irradiation, irradiance, daily broadband atmospheric transmittance (clearness index), monthly mean of daily irradiation, irradiance over a month, 5-day irradiation, 10-day irradiation, monthly irradiation.

Since the geographical site selected by the customer is usually not one of the sites present in the database, a spatial interpolation is necessary. It is performed by using the interpolation scheme developed in WP 5.1 (deliverable D5-1-1) applied to the closest nine sites in the database. The altitude necessary for performing the interpolation is passed to helio\_gd when it is called by a php script (see next section). This interpolation is performed by helio\_gd. This means that nine time-series are extracted and converted to provide values for a single site. Using the nearest neighbour results in a

fastest answer but less accurate. Anyway, the execution time is fast enough. This property was used for the design of the database.

A reliability parameter is provided with the requested variable. It is assessed from the number of values that were used to compute the variable under concern. Given in five classes, it permits at a glance to gauge the quality of the retrieval. The accuracy (bias, rmse) of the estimates was assessed through comparison with ground measurements for 30 to 90 sites in Europe and Africa and several years. It is reported in the HTML page describing the resource in the SoDa HGSS.

The time system of the database is the UTC one (through the Eumetsat time system). Computations are all made in the True Solar Time system for more accurate results.

### Service Execution

The service execution comprises

- time-space requests, unit conversion, parameter selection, within the SoDa IS;
- invoking the resource in the server *www.helioclim.org*, which launches the application described in the previous section;
- extraction of data contained in the database;
- their conversion to the proper parameter;
- the spatial interpolation, including the call to SoDa for obtaining the terrain elevation for the site under concern;
- the creation of the outputs;
- streaming the outputs back to the SoDa IS.

Requirements about geographical and temporal selection are those already in use in the SoDa GUI (tags <geopoint> and <timeperiod>). Unit selection and variable selection (irradiance, irradiation, broadband transmittance) are performed through the service additional GUI.

The server is based on Apache that contains an ODBC (Open Database Connectivity) driver and is already containing some resources of the SoDa service. The resource is invoked through an HTTP Get request (see the XML resource description). The outputs of the resource are written according the SoDa XML guidelines.

Figure 4 depicts the inputs, outputs and the resources called in the service execution.

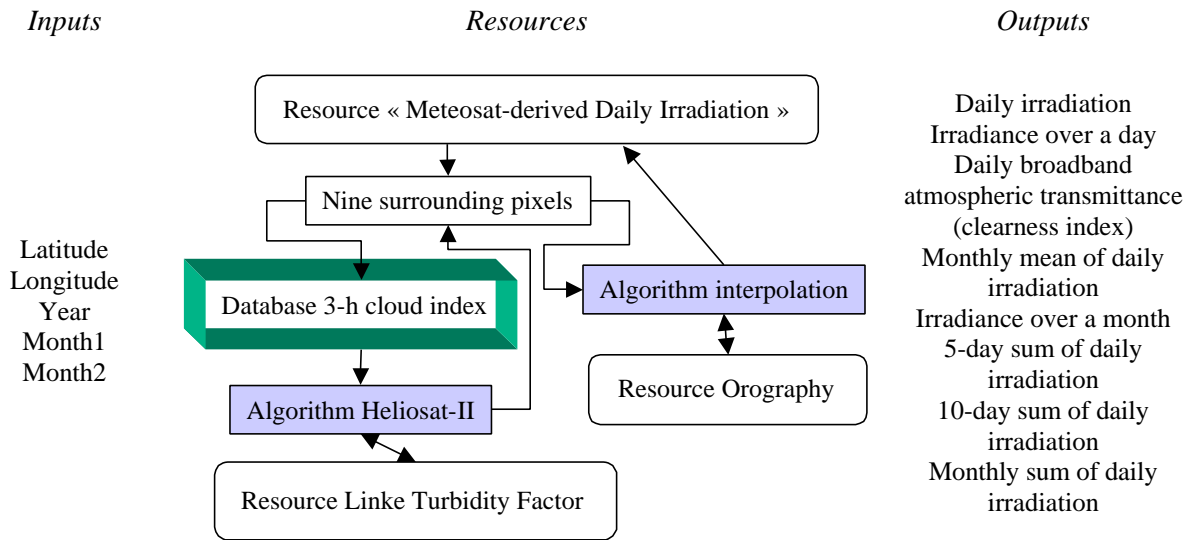


Figure 4.

The execution is performed in three embedded levels. The first level is that invoked by the SoDa IS (heliogd.php, see the resource description). It obtains the inputs from the GUI as well as the site altitude by invoking the appropriate SoDa resource. It then calls the second level, which is also a PHP script (helio\_run.php). This script performs additional tasks and launches the third level: helio\_gd.exe. Each level returns to the upper level, the first level returning to the SoDa IS. The major rationale for selecting such a hierarchy is the independency between the components, which permits to develop, test, update, modify one of them, modify the SoDa XML, etc., without changing the whole application.

Resource description:

```
<?xml version="1.0"?>
<resource>
  <info>
    <name>Meteosat-derived Daily Irradiation – Europe / Africa</name>
    <producer>Ecole des Mines de Paris</producer>
    <url>http://www.helioclim.net/com/heliogd.php</url>
  </info>
  <input parameter="varid" type="numeric" dimension="single">
    <show>Select the parameter to extract</show>
    <list>
      <option default="true" value="1">Daily irradiation</option>
      <option value="2">Irradiance over a day</option>
      <option value="3">Daily broadband atmospheric transmittance (clearness
index)</option>
      <option value="4">Monthly mean of daily irradiation</option>
```

```
<option value="5">Irradiance over a month</option>
<option value="6">5-day sum of daily irradiation</option>
<option value="7">10-day sum of daily irradiation</option>
<option value="8">Monthly sum of daily irradiation </option>
</list>
</input>
<input parameter="latlon" type="geopoint" dimension="single">
  <show>Select on the map the point of interest</show>
</input>
<input parameter="period" type="timeperiod" dimension="single">
  <timerange>1985-01-01,19997-12-31</timerange>
  <show>Enter the period (first day, last day, same year)</show>
</input>
</resource>
```

## References

- Angles J., Menard L., Bauer O., Wald L., 1998, A Web server for accessing a database on solar radiation parameters. In Proceedings of the Earth Observation & Geo-Spatial Web and Internet Workshop '98, Josef Strobl & Clive Best Eds., Salzburger Geographische Materialien, Universität Salzburg, Salzburg, Austria, Heft 27, 33-34.
- Angles J., Menard L., Bauer O., Rigollier C., Wald L., 1999, A climatological database of the Linke turbidity factor. In Proceedings of the ISES Solar World Congress 1999, Jerusalem, Israel, July 4-9, 1999, volume I, 432-434.
- Anonymous, 1996, *The Meteosat Archive, Format Guide No. 3, ISCCP Data Set (IDS) in OpenMTP Format*, February 1996, EUM FG3, Rev. 1.0, Published by Eumetsat, Darmstadt, Germany.
- Bauer O., 1996, Les échanges océan-atmosphère dans l'Atlantique subtropical nord-est : apports de Meteosat. Thèse de Doctorat, Université de Nice - Sophia Antipolis, 162 p.
- Beyer H.G., Costanzo C., Heinemann D., 1996, Modifications of the Heliosat procedure for irradiance estimates from satellite images. *Solar Energy*, **56**, 3, 207-212.
- Beyer H. G., Reise C. and Wald L., 1992. Utilization of satellite data for the assessment of large scale PV grid integration. In *Proceedings of 11th Photovoltaic Solar Energy Conference*, pp. 1309-1312, Hardwood Academic Publ., Switzerland.
- Beyer H.G., Wald L., 1996, Merging ground-measurements and satellite-derived data for the construction of global radiation map. In Proceedings of the conference « Fusion of Earth data: merging point measurements, raster maps, and remotely sensed images », Cannes, France, February 6-8, 1996, Thierry Ranchin and Lucien Wald Editors, published by SEE/URISCA, Nice, France, 37-43.
- Beyer H.-G., Czeplak G., Terzenbach U., Wald L., 1997, Assessment of the method used to construct clearness index maps for the new european solar radiation atlas (ESRA). *Solar Energy*, 61, 6, 389-397.
- Cano D., 1982, Etude de l'enneigement par analyse de séquences d'images de satellite. Application à l'évaluation du rayonnement solaire global au sol. Thèse de Doctorat, École Nationale Supérieure des Télécommunications, Paris, France.
- Cano D., Monget J.M., Albuissou M., Guillard H., Regas N., and Wald L., 1986, A method for the determination of the global solar radiation from meteorological satellite data, *Solar Energy*, **37**, 31-39.
- CERES, 1999. Clouds and the Earth's Radiant Energy System. CD-ROM, CERES ES-4 & ES-9, available at NASA Langley Distributed Active Archive Center, Hampton, Virginia, USA. <http://asd-www.larc.nasa.gov/ceres/ASDceres.html>
- Colle S., Luna de Abreu S., Couto P., Mantelli S., 1999, Distribution of solar irradiation in Brazil derived from geostationary satellite data, In Proceedings of the Solar World Congress ISES 1999 (CD-ROM), Jerusalem, July 4-9 1999.
- Costanzo C., 1994, Bestimmung der solaren Einstrahlung am Boden aus Meteosat-Daten-Untersuchung und Erweiterung einer empirischen Methode. Diploma thesis, Physic Dept., Carl von Ossietzky University, Oldenburg, Germany.
- Delorme C., Gallo A., and Olivieri J., 1992, Quick use of Wefax images from Meteosat to determine daily solar radiation in France, *Solar Energy*, **49** (3), 191-197.
- Diabaté L., 1989, Détermination du rayonnement solaire à l'aide d'images satellitaires. Thèse de Doctorat en Sciences, École Nationale Supérieure des Mines de Paris, Paris, France.
- Diabaté L., Demarcq H., Michaud-Regas N., Wald L., 1988a, Estimating incident solar radiation at the surface from images of the Earth transmitted by geostationary satellites: the Heliosat Project, *International Journal of Solar Energy*, **5**, 261-278.

- Diabaté L., Moussu G., Wald L., 1988b, An operational tool for the fine-scale mapping of the incident solar radiation using satellite images : the Heliosat station. In : Proceedings of the 1988 annual meeting of the American Solar Energy Society, pp. 11-17.
- Diabaté L., Moussu G., Wald L., 1989, Description of an operational tool for determining global solar radiation at ground using geostationary satellite images, *Solar Energy*, **42**, 201-207.
- Diabaté L., Michaud-Regas N., Wald L., 1989, Mapping the ground albedo of Western Africa and its time evolution during 1984 using Meteosat visible data, *Remote Sensing of Environment*, **27**, 3, 211-222.
- DLR – DFD (The German Remote Sensing Center. <http://www.dfd.dlr.de/>)
- Dogniaux R., Lemoine M., 1983, Classification of radiation sites in terms of different indices of atmospheric transparency. In Palz W. (éditeur), *Solar Energy R&D in the European Community*, Series F, Vol. 2, Solar Energy Data. D. Reidel Publ. Co., Dordrecht, 94-107.
- Dumortier D., 1995, Modelling global and diffuse horizontal irradiances under cloudless skies with different turbidities. Final report JOU2-CT92-0144, Daylight II, Ecole Nationale des Travaux Publics de l'Etat, France.
- Earth observation by Meteosat, 1993. Six years of observation of the Earth and its environment by Meteosat, January 1986 – December 1991, CD-ROM, available at European Space Agency, Paris, France.
- EEA-EIONET. <http://www.eionet.eu.int/>
- Environment Canada. Canadian Climate and Water Information. [http://www.msc-smc.ec.gc.ca/climate/index\\_e.cfm](http://www.msc-smc.ec.gc.ca/climate/index_e.cfm)
- ESRA, *European Solar Radiation Atlas*, 1984. Second and Extended Edition, Vols I et II. Edited by Palz W., Commission of the European Communities, DG Science, Research and Development, Report N° EUR 9344, Bruxelles.
- ESRA, *European Solar Radiation Atlas*, 2000. Fourth edition, includ. CD-ROM. Edited by J. Greif, K. Scharmer. Scientific advisors: R. Dogniaux, J. K. Page. Authors: L. Wald, M. Albuissou, G. Czeplak, B. Bourges, R. Aguiar, H. Lund, A. Joukoff, U. Terzenbach, H. G. Beyer, E. P. Borisenko. Published for the Commission of the European Communities by Presses de l'Ecole, Ecole des Mines de Paris, Paris, France.
- EUMETNET-European Climate Data Set, 2001. CD-ROM, version 1, November 2001, available at KNMI, The Netherlands.
- Fontoynt M., Dumortier D., Heinemann D., Hammer A., Olseth J.A., Skarveit A., Ineichen P., Reise C., Page J., Roche L., Beyer H.G., Wald L., 1997, Satel-Light, Processing of Meteosat data for the production of high quality daylight and solar radiation data available on a World Wide Web Internet server, Mid-term progress report JOR3 - CT 95 - 0041, Project Satel-Light, for the Commission of the European Communities, Ecole Nationale des Travaux Publics de l'Etat, Vaulx-en-Velin, France.
- Global Daily Summary, 1994. Temperature and precipitation 1977 – 1991. CD-ROM, version 1, March 1994, available at NOAA National Climatic Data Center, Asheville, NC, USA.
- Global-Land 1-km AVHRR. Vegetation Index June 21-30, 1992. CD-ROM available at Land Processes Distributed Active Archive Center, EROS Data Center, Sioux Falls, South Dakota, USA.
- Global Upper Air Climatic Atlas, 1993. CD-ROM, version 1.0, April 1993, vol. 1: 1980 – 1987, vol. 2: 1985 – 1991, available at NOAA National Climatic Data Center, Asheville, NC, USA.
- Grüter W., Guillard H., Möser W., Monget J.M., Palz W., Raschke E., Reinhardt R.E., Schwarzmann P., Wald L., 1986, Solar Radiation Data from Satellite Images, *Solar Energy R&D in the European Community*, Series F, Volume 4, D. Reidel Publishing Company, 100 p.
- Hammer A., Heinemann D., Westerhellweg A., 1997a, Normalisation of Meteosat counts - an investigation basing on ocean pixels, Satel-Light project for the Commission of the European Communities. Carl von Ossietzky University, Oldenburg, Germany.

- Hammer A., Degner T, Heinemann D., Westerhellweg A., 1997b, Modifications of the Heliosat method cloud index improvements, detection of snow cover and results of radiative transfer calculations, Satel-Light project for the Commission of the European Communities. Carl von Ossietzky University, Oldenburg, Germany.
- Hay J.E., 1981, The mesoscale distribution of solar radiation at the Earth's surface and the ability of satellites to resolve it, In Proceedings of the First Workshop on Terrestrial Solar Resource Forecasting and on Use of Satellites for Terrestrial Solar Resource Assessment, Washington D.C., February 2-5 1981.
- Hay J.E., 1984, An assessment of the mesoscale variability of solar radiation at the Earth's surface, *Solar Energy*, **32**, 425-434.
- Hay J.E., Hanson K.J., 1985, Evaluating the solar resource: a review of problems resulting from temporal, spatial and angular variations, *Solar Energy*, **34**, 151-161.
- Heidt F.D., Teichmann C., Büchler P., Schulze-Kegel D., 1998, Satellite-based solar radiation data go Internet, In Proceedings of the second ISES-Europe Solar Congress, EuroSun'98.
- HelioClim. <http://www.helioclim.org>
- Hulme M., Conway D., Jones P.D., Jiang T., Barrow E.M., Turney C., 1995, A 1961-90 climatology for Europe for climate change modelling and impact applications, *International Journal of Climatology*, **15**, 1333-1363.
- Iehlé A., Lefèvre M., Bauer O., Martinoli M., and Wald L., 1997, Meteosat: A valuable tool for agrometeorology, Final report for the European Commission, Joint Research Centre, Ispra, Italy.
- IFREMER-SISMER. <http://www.ifremer.fr/sismer/>
- Ineichen P., Perez R., 2000, Derivation of cloud index from geostationary satellites and application to the production of solar irradiance and daylight illuminance data, *Theoretical and Applied Climatology*, **64**, 119-130.
- INFEO. Information on Earth Observation. <http://www.infeo.org/>
- IPCC Data Distribution Centre (International Panel on Climate Change). Providing Climate Change and Related Scenarios for Impact Assessments. CD-ROM, version 1, April 1999, available at IPCC Secretariat, Geneva. <http://ipcc-ddc.cru.uea.ac.uk>
- ISCCP. International Satellite Cloud Climatology Project Data. Monthly Cloud Products: July 1983 – December 1988 and January 1989 – December 1993. CD-ROM ISCCP D2, available at NASA Langley Distributed Active Archive Center, Hampton, Virginia, USA. <http://www.cira.colostate.edu/climate/isccp/jisccp2/jisccp2.htm>
- ISLCP. International Satellite Land Surface Climatology Project. Global Data Sets for Land-Atmosphere Models. CD-ROM, vols 1-5: 1987 – 1988, March 1995, available at NASA DAAC Goddard Space Flight Center, Maryland, USA.
- Kasten F., 1996, The Linke turbidity factor based on improved values of the integral Rayleigh optical thickness. *Solar Energy*, **56**, 239-244.
- Kasten F., 1990, Höhenabhängigkeit der Globalstrahlung bei wolkenlosem Himmel, personal communication between Kasten F., DWD, and Zelenka A., Swiss Meteorological Institute.
- Kasten F. and Young A.T., 1989, Revised optical air mass tables and approximation formula. *Applied Optics*, **28** (22), 4735-4738.
- Kneizys F. X., Abreu L.W., Anderson G.P., Chetwynd J.H., Shettle E.P., Berk A., Bernstein L.S., Robertson D.C., Acharya P., Rothman L.S., Selby J.E.A., Galery W.O., Cough S.A., 1996, The MODTRAN 2 / 3 Report and LOWTRAN 7 Model. Technical report, Phillips Laboratory, Geophysics Directorate, Hanscom AFB.
- Lefèvre M., Bauer O., Iehlé A., Wald L., 2000, An automatic method for the calibration of time-series of Meteosat images, *International Journal of Remote Sensing*, **21** (5), 1025-1045.
- Maxwell E. L., 1998, Metstat - The solar radiation model used in the production of the national solar radiation data base (NSRDB), *Solar Energy*, **62**(4), 263-279.
- MedAtlas. <http://www.meteo.ru/nodc/project/project.htm>

- Medias-France, 1994. Mediterranean Oceanic Database – Satellite data and meteorological model outputs. CD-ROM, available at Medias-France, Toulouse, France.
- Meteonorm, 1997, Remund J., Kunz S., *Meteonorm version 3.0, Global meteorological database for solar energy and applied climatology*, Nova Energie GmbH, Schachenallee 29, CH-5000 Aarau, Switzerland.
- Meteonorm, 2000, Remund J., Kunz S., Lang R., *Meteonorm version 4.0, Global meteorological database for solar energy and applied climatology*, Nova Energie GmbH, Schachenallee 29, CH-5000 Aarau, Switzerland.
- Meteosat Collection. CD-ROMs available at European Space Agency, Paris, France.
- Michaud-Regas N., 1986, Mise en oeuvre et validation d'une méthode opérationnelle et automatique pour l'évaluation d'atlas solaires en Europe à l'aide de mesures satellitaires Meteosat. Thèse de Doctorat, Université Paris VII, Paris, France.
- MODB (The Mediterranean Oceanic Database). <http://modb.oce.ulg.ac.be/>
- Molineaux B., Ineichen P., Delauney J.J., 1995, Direct luminous efficacy and atmospheric turbidity – improving model performance, *Solar Energy*, **55** (2), 125-137.
- Möser W., Raschke E., 1983, Mapping of global radiation and of cloudiness from Meteosat image data: theory and ground truth comparisons, *Meteorologische Rundschau*, **36**, 33-41.
- Möser W., Raschke E., 1984, Incident solar radiation over Europe estimated from Meteosat data, *Journal of Applied Meteorology*, **23**, 166-170.
- Moussu G., Diabaté L., Obrecht D., Wald L., 1989, A method for the mapping of the apparent ground brightness using visible images from geostationary satellites, *International Journal of Remote Sensing*, **10** (7), 1207-1225.
- NASA-EO Newsroom. <http://earthobservatory.nasa.gov/Newsroom/NewImages/>
- NASA-EOSDIS (Earth Observing System Data and Information System). [http://eospsso.gsfc.nasa.gov/eos\\_homepage/scientists.html](http://eospsso.gsfc.nasa.gov/eos_homepage/scientists.html)
- NASA-JPL DAAC. Physical Oceanography Distributed Active Archive Center. <http://podaac.jpl.nasa.gov/>
- NASA-LARC. Live Access to Climate Data. [http://asd-www.larc.nasa.gov/cgi-bin/climate\\_server](http://asd-www.larc.nasa.gov/cgi-bin/climate_server)
- NASA-LARC. Surface Meteorology and Solar Energy Data Set. <http://eosweb.larc.nasa.gov/sse/>
- NASA-SAGE. Stratospheric Aerosol Measurement II: October 1978 – January 1993. CD-ROM, available at NASA Langley Distributed Active Archive Center, Hampton, Virginia, USA.
- NASA-SRB. First WCRP Surface Radiation Budget Global Data Sets. Shortwave Radiation Parameters March 1985 – December 1988. CD-ROM, version 1.1, available at NASA Langley Distributed Active Archive Center, Hampton, Virginia, USA.
- NASA Web site for Atmospheric Chemistry and Solar Radiation. [http://www.earth.nasa.gov/science/Science\\_atmosphere.html](http://www.earth.nasa.gov/science/Science_atmosphere.html)
- Neckel, H., and D. Labs, 1984, The solar radiation between 3300 and 12500 Å. *Solar Physics*, **90**, 205-258.
- NOAA – NCDC. <http://lwf.ncdc.noaa.gov/oa/ncdc.html>
- NREL (National Renewable Energy Laboratory). Solar Radiation Resource Information. <http://rredc.nrel.gov/solar/>
- Obrecht D., 1990, Météorologie solaire et images satellitaires : cartographie du rayonnement solaire, détermination de l'albédo des sols et évaluation de l'enneigement. Thèse de Doctorat en Sciences, Université de Nice- Sophia Antipolis, France.
- Pastre C., 1981, Développement d'une méthode de détermination du rayonnement solaire global à partir des données Meteosat, *La Météorologie*, VI<sup>e</sup> série N°24, mars 1981.
- Perez R., Seals R., Zelenka A., 1997, Comparing satellite remote sensing and ground network measurements for the production of site/time specific irradiance data, *Solar Energy*, **60**, 89-96.
- Perrin de Brichambaut C., Vauge C., 1982, *Le gisement solaire : Evaluation de la ressource énergétique*, Paris: Technique et documentation (Lavoisier).

- Pinker R. T. and Laszlo I., 1991. Effects of spatial sampling of satellite data on derived surface solar irradiance. *Journal of Atmospheric and Oceanic Technology*, **8**, 1, 96-107.
- Raschke E., Stuhlmann R., Palz W., Steemers T.C., 1991, *Solar Radiation Atlas of Africa*. Published for the Commission of the European Communities by A. Balkema, Rotterdam, 155 p.
- Remund J., Page J., 2002, Advanced parameters. Chain of algorithms: short- and longwave radiation with associated temperature prediction resources. Report to the European Commission, SoDa (Integration and exploitation of networked Solar radiation Databases for environment monitoring) project IST-1999-12245, 72 p. (see online at <http://soda.jrc.it>).
- RETScreen. <http://retscreen.gc.ca/>
- Rigollier C., 2000, Vers un accès à une climatologie du rayonnement solaire : estimation de l'irradiation globale à partir d'images satellitales. Thèse de Doctorat en Sciences et Technologies de l'Information et de la Communication, Université Nice – Sophia Antipolis, France, 194 p.
- Rigollier C., Bauer O., Wald L., 2000, On the clear sky model of the 4th European Solar Radiation Atlas with respect to the Heliosat method, *Solar Energy*, **68** (1), 33-48.
- Rigollier C., Lefèvre M., Blanc Ph., Wald L., 2002. The operational calibration of images taken in the visible channel of the Meteosat-series of satellites. *To be published by Journal of Atmospheric and Oceanic Technology*.
- Rigollier C., Wald L., 1999, The HelioClim Project: from satellite images to solar radiation maps. In *Proceedings of the ISES Solar World Congress 1999*, Jerusalem, Israel, July 4-9, 1999, volume I, pp 427-431.
- Satel-Light. <http://www.satel-light.com/>
- Schiffer, R.A. and Rossow, W.B., 1983, The International Satellite Cloud Climatology Project (ISCCP): The first project of the World Climate Research Programme. *Bulletin American Meteorological Society*, **64**, 779-784.
- Schiffer, R.A. and Rossow, W.B., 1985, ISCCP global radiance data set: A new resource for climate research. *Bulletin American Meteorological Society*, **66**, 1498-1503.
- Stuhlmann R., Rieland M., Raschke E., 1990, An improvement of the IGMK model to derive total and diffuse solar radiation at the surface from satellite data, *Journal of Applied Meteorology*, **29**, 596-603.
- Supit I., 1994, Global radiation. Agriculture series, EUR 15745, European Commission, Office for Official Publications, Luxembourg, 194 p.
- SWERA. Solar and Wind Resource Assessment. <http://swera.unep.net/>
- SWITCH. Solar Water Integrated Thermal Cooling and Heating Systems. <http://fernande.cma.fr/switch/>
- Tanré D., Deroo C., Duhaut P., Herman M., Morcrette J.J., Perbos J., Deschamps P.Y., 1990, Description of a computer code to simulate the satellite signal in the solar spectrum: the 5S code, *International Journal of Remote Sensing*, **11**(4), 659-668.
- Taylor V.R., Stowe L.L., 1984a, Reflectance characteristics of uniform Earth and cloud surfaces derived from Nimbus 7 ERB, *Journal of Geophysical Research*, **89**(D4), 4987-4996.
- Taylor V.R., Stowe L.L., 1984b, Atlas of reflectance patterns for uniform Earth and cloud surfaces (Nimbus 7 ERB – 61 days), NOAA Technical Report NESDIS 10, July 1984, Washington, DC, USA.
- Unidata. <http://www.unidata.ucar.edu/>
- USGS (United States Geological Survey). <http://www.usgs.gov/>
- Vermote E., Tanré D., Deuzé J.L., Herman M., Morcrette J.J., 1994, Second Simulation of the Satellite Signal in the Solar Spectrum (6S), 6S User Guide, NASA-Goddard Space Flight Center - Code 923, Greenbelt, USA.
- Wald L., Monget J.M., 1983a, Sea surface winds from sun glitter observations. *Journal of Geophysical Research*, **88**, C4, 2547-2555.

- Wald L., Monget J.M., 1983b, Remote sensing of the sea-state using the 0.8-1.1 microns channel. *International Journal of Remote Sensing*, 4, 2, 433-446, 1983. Comments by P. Koepke and reply, 6, 5, 787-799, 1985.
- Wald L., Wald J.-L., Moussu G., 1992, A technical note on a low-cost high-quality system for the acquisition and digital processing of images of WEFAX type provided by meteorological geostationary satellites. *International Journal of Remote Sensing*, 13, 5, 911-916.
- World Meteorological Organization (WMO), 1981, Meteorological aspects of the utilization of solar radiation as an energy source. Annex: World maps of relative global radiation. Technical Note N° 172, WMO-N° 557, Geneva, Switzerland, 298 pp.
- WMO-CLINO, 1998. Global Climate Normals (CLINO) 1961 – 1990. CD-ROM, version 1, November 1998, available NOAA National Climatic Data Center, Asheville, NC, USA.
- WMO Online Satellite Imagery Sites. <http://www.wmo.ch/hinsman/imagery.html>
- WMO – World Radiation Data Center. [http://wrdc.mgo.rssi.ru/Lefts\\_en.htm](http://wrdc.mgo.rssi.ru/Lefts_en.htm)
- Zelenka A., Czeplak G., d’Agostino V., Josefson W., Maxwell E., Perez R., 1992, Techniques for supplementing solar radiation network data, Technical Report, International Energy Agency, # IEA-SHCP-9D-1, Swiss Meteorological Institute, Krahbühlstrasse, 58, CH-8044 Zurich, Switzerland.
- Zelenka A., Perez R., Seals R., and Renné D., 1999, Effective accuracy of satellite-derived hourly irradiances, *Theoretical and Applied Climatology*, **62**, 199-207.

## Annex A. Notations

The following notations are employed in this document.

The following subscripts are used

- $0$ : extraterrestrial or astronomical values,
- $g$ : ground related values,
- $c$ : clear sky (*i.e.* cloudless sky) values,
- $b$ : overcast sky values.
- $I$ : spectral values.

### **Astronomical quantities and sun angles**

- $t$  is the time.
- $q_s$  is the sun zenithal angle.
- $g_s$  is the sun elevation at time  $t$ , also called the solar altitude angle.  $g_s$  is  $0^\circ$  at sunrise and sunset.  $q_s = \pi/2 - g_s$ .
- $I_0$  is the solar constant, that is the extraterrestrial irradiance normal to the solar beam at the mean solar distance. It is equal to  $1367 \text{ W}\cdot\text{m}^{-2}$ .
- $I_{0I}$  is the spectral distribution of solar radiation outside the atmosphere. It is created by averaging or interpolating values read in published tables, to irradiance for 10 nm intervals centred on the indicated wavelengths. These tables are those of Neckel, Labs (1984), read from Justus (1989) and Rossow *et al.* (1992). Units are  $\text{W m}^{-2} \mu\text{m}^{-1}$ .
- $e$  is the correction used to allow for the variation of sun-earth distance from its mean value. It depends upon the day.  $I_0 e(t)$  is the extraterrestrial irradiance for the current day observed on a surface normal to the solar beam.
- $d$  is the declination (positive when the sun is north to the equator: March 21 to September 23). Maximum and minimum values of the declination are  $+23^\circ 27'$  and  $-23^\circ 27'$ .
- $Dl$  is the length of the day, *i.e.* 24 hours or 86400 seconds.
- the solar hour angle,  $w$ , expresses the time of the day in terms of the angle of rotation of the Earth about its axis from its solar noon position at a specific place. As the Earth rotates of  $360^\circ$  (or  $2\pi$  rad) in 24 hours, in one hour the rotation is  $15^\circ$  (or  $\pi/12$  rad). Given an instant  $t$  in true solar time (TST) expressed in decimal hour,  $w = (t-12)\pi/12$ . If  $t$  is Universal Time (UT) in decimal hour, if  $I$  is the longitude (positive eastwards) and if  $Dt$  is the correction of time (the so-called equation of time) in decimal hour, then  $w = \pi/12 (t + 12I/\pi + Dt - 12)$ , if  $I$  is in radians, or  $w = 15 (t + I/15 + Dt - 12)$  if  $I$  is expressed in degrees.

### **Radiation quantities**

The letters  $L$ ,  $G$ ,  $D$ ,  $I$  and  $B$  denote the following quantities:

- $L$ : radiance ( $\text{W m}^{-2} \text{sr}^{-1}$ ),
- $G$ : global irradiance or irradiation,

- $D$ : diffuse irradiance or irradiation (diffuse component of solar radiation),
- $I$ : normal direct irradiance or irradiation (beam component of solar radiation normal to the direction of the sun),
- $B$ : direct irradiance or irradiation (beam component of solar radiation).

The basic time intervals to which the irradiation values refer are identified by the following subscripts:

- $h$ : hourly values (e.g., the integral of the global irradiance observed during one hour, which is the hourly irradiation),
- $d$ : daily values (e.g., the integral of the global irradiance observed during one day, which is the daily irradiation),
- $m$ : mean monthly values (e.g., the mean value of the hourly irradiation observed during one month for the hour  $h$ ).

Notations for the irradiances and irradiations:

- $G_o^t(i,j)$  is the horizontal irradiance outside the atmosphere for the time  $t$  and the pixel  $(i, j)$ .  $G_o^t(i,j) = I_o \mathbf{e}(t) \sin \mathbf{g}(t,i,j)$ . It is expressed in  $\text{W m}^{-2}$ .
- $G_{oh}(i,j)$  is the horizontal hourly irradiation outside the atmosphere for the hour  $h$  and the pixel  $(i, j)$ . It is expressed in  $\text{W h m}^{-2}$ .
- $G_{od}(i,j)$  is the horizontal daily irradiation outside the atmosphere for the day  $d$  and the pixel  $(i, j)$ . It is expressed in  $\text{W h m}^{-2}$ .
- $G^t(i,j)$ ,  $B^t(i,j)$  and  $D^t(i,j)$  are respectively the horizontal global, beam and diffuse irradiances at ground level for the time  $t$  and the pixel  $(i, j)$ . They are expressed in  $\text{W m}^{-2}$ .
- $G_c^t(i,j)$ ,  $B_c^t(i,j)$  and  $D_c^t(i,j)$  are respectively the horizontal global, beam and diffuse irradiances at ground level under clear sky for the time  $t$  and the pixel  $(i, j)$ . They are expressed in  $\text{W m}^{-2}$ .
- $G_h(i,j)$ ,  $B_h(i,j)$  and  $D_h(i,j)$  are respectively the horizontal global, beam and diffuse hourly irradiations at ground level for the hour  $h$  and the pixel  $(i, j)$ . They are expressed in  $\text{W h m}^{-2}$ . Similar notations hold for the daily irradiations, with a subscript  $d$ .
- $G_{ch}(i,j)$ ,  $B_{ch}(i,j)$  and  $D_{ch}(i,j)$  are respectively the horizontal global, beam and diffuse hourly irradiations at ground level under clear sky for the hour  $h$  and the pixel  $(i, j)$ . They are expressed in  $\text{W h m}^{-2}$ . Similar notations hold for the daily irradiations, with a subscript  $d$ .

### Notations for describing the optical properties of the atmosphere and the ground

- $KT^t(i,j)$  is the clearness index for the time  $t$  and the pixel  $(i, j)$ . It is equal to the ratio of the global radiation at ground on a horizontal surface  $G^t(i,j)$  to the horizontal radiation outside the atmosphere  $G_o^t(i,j)$ :  $KT^t(i,j) = G^t(i,j) / G_o^t(i,j)$ . The clearness index may be defined from irradiance or from hourly or daily irradiations:  $KT_h(i,j)$  or  $KT_d(i,j)$ .
- $K_c^t(i,j)$  is the clear-sky index for the time  $t$  and the pixel  $(i, j)$ . It is equal to the ratio of the global radiation at ground on a horizontal surface  $G^t(i,j)$  to the same quantity but for clear skies  $G_c^t(i,j)$ :  $K_c^t(i,j) = G^t(i,j) / G_c^t(i,j)$ . It may be defined from irradiance or from hourly or daily irradiations:  $K_{ch}(i,j)$  or  $K_{cd}(i,j)$ .
- $T_L(AM2)$  is the Linke turbidity factor for a relative air mass  $m$  equal to 2.

- $m$  is the relative optical air mass. It expresses the ratio of the optical path length of the solar beam through the atmosphere to the optical path through a standard atmosphere at sea level with the sun at the zenith.
- $d_R(m)$  is the integral Rayleigh optical thickness.
- $L^t(i,j)$  is the radiance observed by the spaceborne for the time  $t$  and the pixel  $(i, j)$ . It is expressed in  $W m^{-2} st^{-1}$ .

### Notations for other properties of the site

- $z$  is the elevation of the site above mean sea level.
- $p$  is the pressure at site elevation and  $p_0$  is the mean atmospheric pressure at sea level.
- $F$  and  $I$  are respectively the latitude (positive to the Northern Hemisphere) and longitude of the site (positive eastwards).

### Satellite (Meteosat) -related quantities

- $S_I$  is the sensor spectral response in the visible range, covering approximately the interval  $[0,3 \mu m, 1,1 \mu m]$  for Meteosat (unitless)
- $I_{0met}$  is the total irradiance in the visible channel for the various Meteosat sensors (*i.e.*  $\int_{0.3}^{1.1} I_{0I} S_I dI$ ), in  $W m^{-2}$
- $r^t(i,j)$  is the apparent albedo observed by the spaceborne sensor for the pixel  $(i, j)$ . It has no unit and is equal to the bidimensional reflectance, assuming the Lambertian hypothesis.  

$$r^t(i,j) = \frac{\mathbf{p} L^t(i,j)}{I_{0met} \mathbf{e}(t) \sin \mathbf{g}_s(t,i,j)} = \frac{\mathbf{p} L^t(i,j)}{I_{0met} \mathbf{e}(t) \cos \mathbf{q}_s(t,i,j)}$$
- $r^t_{cloud}(i,j)$  is the apparent albedo observed by the spaceborne sensor over the brightest clouds for the pixel  $(i, j)$  (unitless) (a quantity specific to the method Heliosat)
- $r^t_g(i,j)$  is the apparent albedo observed by the spaceborne sensor over the ground under clear skies for the pixel  $(i, j)$  (unitless) (a quantity specific to the method Heliosat)
- $q_v$  is the viewing angle, equal to zero when looking to nadir
- $y$  is the difference between the sun and satellite azimuth angles
- $a^t, b^t$  and  $CN^t_{dark}$  are the calibration coefficients of the Meteosat radiometer at instant  $t$ .

## Annex B. Overview of the method Heliosat-II

The principle of the method Heliosat-II, as well as most current methods, is that a difference in global radiation perceived by the sensor aboard the satellite is only due to a change in apparent albedo, which is itself due to an increase of the radiation emitted by the atmosphere towards the sensor.

A key parameter is the cloud index  $n$ , resulting from a comparison of what is observed by the sensor to what should be observed over that pixel if the sky were clear, which is related to the "clearness" of the atmosphere. In principle, it can be written as:

$$n^t(i,j) = [ \mathbf{r}^t(i,j) - \mathbf{r}_g^t(i,j) ] / [ \mathbf{r}_{cloud}^t - \mathbf{r}_g^t(i,j) ]$$

where

- $\mathbf{r}^t(i,j)$  is the reflectance, or apparent albedo, observed by the spaceborne sensor for the time  $t$  and the pixel  $(i, j)$ :  $\mathbf{r}^t(i,j) = \frac{\mathbf{p} L^t(i,j)}{I_{0met} \mathbf{e}(t) \cos \mathbf{q}_S(t,i,j)}$ , where  $L^t(i,j)$  is the observed radiance,
- $\mathbf{r}_{cloud}^t(i,j)$  is the apparent albedo over the brightest clouds,
- and  $\mathbf{r}_g^t(i,j)$  is the apparent albedo over the ground under clear skies.

If the sky is clear, the apparent albedo  $\mathbf{r}^t(i,j)$  is close to the apparent albedo over the ground and the cloud index  $n$  is close to 0 (possibly negative). If the sky is overcast, the cloud index  $n$  is close to 1 (possibly larger). In brief, the cloud index  $n$  may be considered as describing the attenuation of the atmosphere (1 minus the transmittance). Thus, the cloud index  $n$ , or similar quantities depending upon the methods, is a very convenient tool to exploit satellite images.

The basic principle is not always verified. Other parameters may intervene, such as multiple cloud layers and dramatic changes in the ground albedo due to the snowfall or the shadow created by a neighbouring cloud. The change in sensor outputs is not necessarily linked to a change in the optical state of the atmosphere or a change in the optical state does not necessarily translate into a change in the cloud index.

The cloud index should not be confused with the cloud cover. Given an overcast sky, the observer at ground level will report a cloud cover of 8 in okta. This cloud cover will be the same whether there is one single layer of clouds or more, while the cloud index  $n$  may be sensitive to the vertical profile of clouds.

The albedos used in the above equation may be constructed from a time-series of satellite images. The optical state of the clear sky is given by a model, often in the form of the global irradiation and its direct and diffuse components and the beam and diffuse transmittances.

Finally, the cloud index  $n$  is related to the global irradiation on an hourly (or half-hourly) basis by the means of the clearness index or the clear-sky index. From these hourly irradiations, the daily irradiation can be constructed.

### Annex C. Modelling the global, direct and diffuse irradiations under clear-skies

Let note the latitude of the site (positive to the Northern Hemisphere),  $F$ , its longitude (positive eastwards),  $L$ , its elevation above mean sea level,  $z$ , the declination of the sun for the day under concern,  $d$ , and the solar hour angle for the instant  $t$ ,  $w$ . The sun elevation above horizon,  $g_s^{true}$ , corrected for refraction is given in radians by:

$$g_s^{true} = g_s + Dg_{refr}$$

$$\sin g_s = \sin F \sin d + \cos F \cos d \cos w$$

$$Dg_{refr} = 0.061359 \frac{0.1594 + 1.123 g_s + 0.065656 g_s^2}{1 + 28.9344 g_s + 277.3971 g_s^2}$$

The modelling of the irradiation for clear skies originates from the clear-sky model of the European Solar Radiation Atlas (ESRA 2000; Rigollier *et al.* 2000) with corrections for the site elevation proposed by Remund, Page (2002).

The relative optical air mass  $m$  expresses the ratio of the optical path length of the solar beam through the atmosphere to the optical path through a standard atmosphere at sea level with the sun at the zenith. As the solar altitude decreases, the relative optical path length increases. The relative optical path length also decreases with increasing site height. A correction procedure is applied, obtained as the ratio of mean atmospheric pressure,  $p$ , at the site elevation, to mean atmospheric pressure at sea level,  $p_0$ . This correction is particularly important in mountainous areas. The relative optical air mass at sea level has no unit and is given by Kasten, Young (1989):

$$m(g_s^{true}) = 1 / [ \sin g_s^{true} + 0.50572 ((180/p)g_s^{true} + 6.07995)^{-1.6364} ]$$

The Rayleigh optical thickness,  $d_R$ , is the optical thickness of a pure Rayleigh scattering atmosphere, per unit of air mass, along a specified path length. As the solar radiation is not monochromatic, the Rayleigh optical thickness depends on the precise optical path and hence on relative optical air mass,  $m$ . The parameterisation used is based on Kasten (1996) and was modified by Remund, Page (2002) to correct the behaviour of the original model with terrain altitude.

The height correction is given by

$$p/p_0 = \exp(-z/z_h)$$

where  $z_h$  is the scale height of the Rayleigh atmosphere near the Earth surface, equal to 8434.5 meters.

Let  $corr\_d_R(p/p_0)$  be the correction of the integral Rayleigh optical thickness due to the elevation of the site. Remund, Page determined this function for two values of  $(p/p_0)$ :

$$corr\_d_R(0.75) = 1.248174 - 0.011997 m(g_s^{true}) + 0.00037 m^2(g_s^{true})$$

$$corr\_d_R(0.50) = 1.68219 - 0.03059 m(g_s^{true}) + 0.00089 m^2(g_s^{true})$$

Given that  $corr\_d_R(1)=1$  and assuming that  $corr\_d_R(p/p_0) = corr\_d_R(0.5)$  for  $(p/p_0)>0.5$ ,  $corr\_d_R(p/p_0)$  can be determined for any  $(p/p_0)$  by piecewise linear interpolation. The integral Rayleigh optical thickness is thus given by:

$$\text{if } m \leq 20, (g_s < 1.9^\circ)$$

$$1/d_R(m) = corr\_d_R(p/p_0) [6.625928 + 1.92969m - 0.170073m^2 + 0.011517m^3 - 0.000285m^4]$$

$$\text{if } m > 20, (g_s < 1.9^\circ), 1/d_R(m) = 10.4 + 0.718 m (p/p_0)$$

## The beam component

The beam irradiation for a period ranging from solar hour angles  $w_1$  to  $w_2$ , is given by:

$$B_c(w_1, w_2) = I_0 e \frac{Dl}{2p} T_{rb}(T_L(AM2)) \int_{w_2}^{w_1} F_b(g_s, T_L(AM2)) dw$$

where

- $e$  is the correction of the variation of sun-earth distance for the day under concern.  $I_0 e$  is the extraterrestrial irradiance for the current day observed on a surface normal to the solar beam.
- $Dl$  is the average length of the day (*i.e.*, 24 hours). The unit of  $B_c$  is  $Wh m^{-2}$  if  $Dl$  is expressed in hours, or  $J m^{-2}$  if  $Dl$  is in seconds.
- $w_1$  to  $w_2$  are related to two instants  $t_1$  and  $t_2$ .

$T_{rb}(T_L(AM2))$  is a transmission function for beam radiation at zenith ( $g_s = p/2$ ), function of the Linke turbidity factor,  $T_L(AM2)$ , and  $F_b$  is a beam angular function.  $B_c$  is set to 0 if the equation leads to a negative value.  $T_{rb}(T_L(AM2))$  and  $F_b(g_s, T_L(AM2))$  are given by:

$$T_{rb}(T_L(AM2)) = exp[-0,8662 T_L(AM2) (p/p_0) d_R(p/p_0)]$$

$$F_b(g_s, T_L(AM2)) = C_0 + C_1 \sin(g_s) + C_2 \sin^2(g_s)$$

The values of the coefficients  $C_0$ ,  $C_1$  and  $C_2$  are polynomials and are given for three ranges of the solar altitude angle at noon,  $g_s^{noon}$ : below  $15^\circ$ , between  $15^\circ$  and  $30^\circ$ , and over  $30^\circ$ :

$$C_0 = L_{00} + L_{01} T_L(AM2) (p/p_0) + L_{02} [T_L(AM2) (p/p_0)]^2$$

$$C_1 = L_{10} + L_{11} T_L(AM2) (p/p_0) + L_{12} [T_L(AM2) (p/p_0)]^2$$

$$C_2 = L_{20} + L_{21} T_L(AM2) (p/p_0) + L_{22} [T_L(AM2) (p/p_0)]^2 + L_{23} [T_L(AM2) (p/p_0)]^3$$

with the  $L_{ij}$  coefficients listed in Table 1. These coefficients, as well as the coefficients  $A_i$ ,  $B_i$ ,  $C_i$  and  $D_i$  (see further) are unitless.

$C_0$	$L_{00}$	$L_{01}$	$L_{02}$
$g_s^{noon} > 30^\circ$	$-1,7349 \cdot 10^{-2}$	$-5,8985 \cdot 10^{-3}$	$6,8868 \cdot 10^{-4}$
$15^\circ < g_s^{noon} \leq 30^\circ$	$-8,2193 \cdot 10^{-3}$	$4,5643 \cdot 10^{-4}$	$6,7916 \cdot 10^{-5}$
$g_s^{noon} \leq 15^\circ$	$-1,1656 \cdot 10^{-3}$	$1,8408 \cdot 10^{-4}$	$-4,8754 \cdot 10^{-7}$
$C_1$	$L_{10}$	$L_{11}$	$L_{12}$
$g_s^{noon} > 30^\circ$	1,0258	$-1,2196 \cdot 10^{-1}$	$1,9229 \cdot 10^{-3}$
$15^\circ < g_s^{noon} \leq 30^\circ$	$8,9233 \cdot 10^{-1}$	$-1,9991 \cdot 10^{-1}$	$9,9741 \cdot 10^{-3}$
$g_s^{noon} \leq 15^\circ$	$7,4095 \cdot 10^{-1}$	$-2,2427 \cdot 10^{-1}$	$1,5314 \cdot 10^{-2}$

	$C_2$	$L_{20}$	$L_{21}$	$L_{22}$	$L_{23}$
$g_s^{noon} > 30^0$		$-7,2178 \cdot 10^{-3}$	$1,3086 \cdot 10^{-1}$	$-2,8405 \cdot 10^{-3}$	0
$15^0 < g_s^{noon} \leq 30^0$		$2,5428 \cdot 10^{-1}$	$2,6140 \cdot 10^{-1}$	$-1,7020 \cdot 10^{-2}$	0
$g_s^{noon} \leq 15^0$		$3,4959 \cdot 10^{-1}$	$7,2313 \cdot 10^{-1}$	$-1,2305 \cdot 10^{-1}$	$5,9194 \cdot 10^{-3}$

**Table 1** Coefficients  $L_{ij}$  for the computation of the  $C_i$  coefficients.

$F_b(g_s, T_L(AM2))$  can be rewritten as a function of  $\mathbf{w}$ ,  $\mathbf{F}$ ,  $\mathbf{d}$ ,  $T_L(AM2)$ :

$$F_b(\mathbf{w}, \mathbf{F}, \mathbf{d}, T_L(AM2)) = B_0 + B_1 \cos \mathbf{w} + B_2 \cos(2\mathbf{w})$$

since

$$\sin g_s = \sin \mathbf{F} \sin \mathbf{d} + \cos \mathbf{F} \cos \mathbf{d} \cos \mathbf{w}$$

It comes

$$B_c(\mathbf{w}_1, \mathbf{w}_2) = I_0 e^{\frac{Dl}{2p}} T_{rb}(T_L(AM2)) [B_0 \mathbf{w} + B_1 \sin(\mathbf{w}) + B_2 \sin(2\mathbf{w})]_{\mathbf{w}_1}^{\mathbf{w}_2}$$

with the coefficients  $B_0$ ,  $B_1$  and  $B_2$  given by:

$$B_0 = C_0 + C_1 \sin(\mathbf{F}) \sin(\mathbf{d}) + C_2 \sin(\mathbf{F})^2 \sin(\mathbf{d})^2 + 0.5 \cos(\mathbf{F})^2 \cos(\mathbf{d})^2$$

$$B_1 = C_1 \cos(\mathbf{F}) \cos(\mathbf{d}) + 2 C_2 \sin(\mathbf{F}) \sin(\mathbf{d}) \cos(\mathbf{F}) \cos(\mathbf{d})$$

$$B_2 = 0.25 C_2 \cos(\mathbf{F})^2 \cos(\mathbf{d})^2$$

The daily integral is achieved by setting  $\mathbf{w}_1$  equal to the sunrise hour angle,  $\mathbf{w}_{SR}$ , and  $\mathbf{w}_2$  to the sunset hour angle,  $\mathbf{w}_{SS}$ , i.e.:

$$B_{cd} = B_c(\mathbf{w}_{SR}, \mathbf{w}_{SS})$$

### The diffuse component

The diffuse horizontal irradiation,  $D_c(\mathbf{w}_1, \mathbf{w}_2)$ , over any period defined by  $\mathbf{w}_1$  and  $\mathbf{w}_2$ , is given by:

$$D_c(\mathbf{w}_1, \mathbf{w}_2) = I_0 e^{\frac{Dl}{2p}} T_{rd}(T_L^*(AM2)) [D_0 \mathbf{w} + D_1 \sin(\mathbf{w}) + D_2 \sin(2\mathbf{w})]_{\mathbf{w}_1}^{\mathbf{w}_2}$$

where  $T_L^*(AM2) = p/p_0 T_L(AM2)$ .

The transmission function at zenith,  $T_{rd}$ , is given by

$$T_{rd}(T_L^*(AM2)) = -1.5843 \cdot 10^{-2} + 3.0543 \cdot 10^{-2} T_L^*(AM2) + 3.797 \cdot 10^{-4} T_L^*(AM2)^2$$

The coefficients  $D_0$ ,  $D_1$  and  $D_2$  are given by:

$$D_0 = A_0 + A_1 \sin(\mathbf{F}) \sin(\mathbf{d}) + A_2 \sin(\mathbf{F})^2 \sin(\mathbf{d})^2 + 0.5 \cos(\mathbf{F})^2 \cos(\mathbf{d})^2$$

$$D_1 = A_1 \cos(\mathbf{F}) \cos(\mathbf{d}) + 2 A_2 \sin(\mathbf{F}) \sin(\mathbf{d}) \cos(\mathbf{F}) \cos(\mathbf{d})$$

$$D_2 = 0.25 A_2 \cos(\mathbf{F})^2 \cos(\mathbf{d})^2$$

The coefficients  $A_0$ ,  $A_1$ , and  $A_2$ , are given by:

$$A_0 = 2,64631 \cdot 10^{-1} - 6,1581 \cdot 10^{-2} T_L^*(AM2) + 3,1408 \cdot 10^{-3} T_L^*(AM2)^2$$

$$A_1 = 2,0402 + 1,89451 \cdot 10^{-2} T_L^*(AM2) - 1,1161 \cdot 10^{-2} T_L^*(AM2)^2$$

$$A_2 = -1,3025 + 3,9231 \cdot 10^{-2} T_L^*(AM2) + 8,5079 \cdot 10^{-3} T_L^*(AM2)^2$$

with a condition on  $A_0$ :

$$\text{if } (A_0 T_{rd}) < 2 \cdot 10^{-3} \text{ then } A_0 = 2 \cdot 10^{-3} / T_{rd}$$

This condition is required because  $A_0$  yields negative values for  $T_L(AM2) > 6$ . It was therefore decided to impose this limiting condition to achieve acceptable values at sunrise and sunset.

The daily integral is achieved by setting  $w_1$  equal to the sunrise hour angle,  $w_{SR}$ , and  $w_2$  to the sunset hour angle,  $w_{SS}$ , *i.e.*

$$D_{cd} = D_c(w_{SR}, w_{SS})$$

### The global irradiation

The global irradiation under clear sky,  $G_c$ , is obtained as the sum of the beam and diffuse horizontal irradiations under clear sky between two instants  $t_1$  and  $t_2$ .

$$G_c(w_1, w_2) = B_c(w_1, w_2) + D_c(w_1, w_2)$$

The parameters  $w_1$  and  $w_2$  are respectively set to  $w_{SR}$  and  $w_{SS}$  for the computation of the daily global irradiation:

$$G_c(w_{SR}, w_{SS}) = B_c(w_{SR}, w_{SS}) + D_c(w_{SR}, w_{SS}) \quad \hat{U} \quad G_{cd} = B_{cd} + D_{cd}$$

One may define the global transmittance of the atmosphere for the incident radiation,  $T(q_s)$ , as the sum of the beam and diffuse transmittances:

$$T(q_s) = Tr_B(q_s) + Tr_D(q_s)$$

## Annex D. The cloud index

The cloud index  $n$  is defined as:

$$n^t(i,j) = [r^t(i,j) - r_g^t(i,j)] / [r_{cloud}^t - r_g^t(i,j)]$$

where

- $r^t(i,j)$  is the reflectance, or apparent albedo, observed by the spaceborne sensor at instant  $t$  and for the pixel  $(i,j)$ :  $r^t(i,j) = \frac{p L^t(i,j)}{I_{0met} e(t) \cos q_s(t,i,j)}$ , where  $L^t(i,j)$  is the observed radiance and  $I_{0met}$  is the total irradiance in the visible channel for the various Meteosat sensors,
- $r_{cloud}^t(i,j)$  is the apparent albedo over the brightest clouds,
- and  $r_g^t(i,j)$  is the albedo over the ground under clear skies.

The computation of  $n^t$  is pending to the determination of the reflectances or albedoes  $r_g^t$  and  $r_{cloud}^t$ . In turn, these reflectances are computed from the analysis of a time-series of the reflectance observed by the sensor  $r^t$ .

The reflectance observed by the sensor  $r^t$  under clear skies is a function of the reflectance of the ground,  $r_g^t$ , the sun zenithal angle,  $q_s$ , the viewing angle,  $q_v$ , and the difference,  $y$ , of the sun and satellite azimuth angles. At the first order, given the large size of the pixel, the multiple reflection and scattering effects are negligible. Assuming a Lambertian ground, the reflectance observed by the sensor is (Tanré *et al.* 1990):

$$r^t(i,j) = r_{atm}^t(q_s, q_v, y) + r_g^t(i,j) T^t(q_s) T^t(q_v)$$

where  $r_{atm}^t(q_s, q_v, y)$  is the intrinsic reflectance of the atmosphere, caused by the scattering of the incident and upward radiation towards the sensor. The parameters  $T^t(q_s)$  and  $T^t(q_v)$  are the global transmittances of the atmosphere for the incident and upward radiation. The principle of reciprocity implies that the same formulation applies to both transmittances.

Numerous works show that the ground is not exactly of Lambertian nature. Vermote *et al.* (1994) propose several bi-directional models to consider these effects in the simulation of  $r^t(i,j)$ . From an operational point of view, the method Heliosat-II cannot consider these effects by lack of information. In particular, it would imply the knowledge of the landuse for each pixel of the field of view of the satellite Meteosat and of the associated model.

The influence of the sun zenithal angle  $q_s$  is important as is that of the Linke turbidity factor, which affects the transmittance. The air mass increases with  $q_s$ , causing an increase of the intrinsic reflectance of the atmosphere  $r_{atm}^t$ . The transmittance decreases as the turbidity increases, or similarly as the visibility decreases. The difference,  $y$ , of the sun and satellite azimuth angles impacts on the reflectance observed by the sensor, though it is less important than the sun zenithal angle.

The present approach is based upon the modelling of the intrinsic reflectance of the atmosphere, also called the path reflectance, and the atmospheric transmittance. Each term,  $r_{atm}^t$  and  $T^t(q_s)$  or  $T^t(q_v)$  is modelled, resulting into the explicit formulation of  $r^t$  as a function of  $q_s$ ,  $q_v$ ,  $y$  and  $r_g^t$ . Inversely, this permits to compute  $r_g^t$  and  $r_{cloud}^t$ .

Assuming that the scattering by the atmosphere is isotropic, it is conceivable that the path radiance  $L_{atm}$  reaching the sensor is proportional to the path radiance reaching the ground. This path radiance can be expressed using the expression of the diffuse irradiance under clear sky at ground level,  $D_c$ :

$$L_{atm} = (D_c / p) (I_{0met} / I_0) (\langle \cos q_v \rangle / \cos q_v)^{0.8}$$

The ratio ( $I_{0met}/I_0$ ) normalises the extraterrestrial irradiance to the Meteosat sensor case. Following Beyer *et al.* (1996), the ratio  $(\langle \cos q_v \rangle / \cos q_v)^{0,8}$  empirically corrects for the viewing angle without bias ( $\langle \cos q_v \rangle = 0,5$ ).

Various tests show that the approach is satisfactory, provided it is restricted to zenithal angles and viewing angles less than  $75^\circ$ , as was the case with the method Heliosat-I (Diabaté 1989; Bauer 1996). It follows that the method Heliosat-II will be unable in principle to accurately estimate the irradiation north of the latitude  $65^\circ$  N, and south of the latitude  $65^\circ$  S.

## Annex E. The computation of the ground albedo

The ground albedo  $\mathbf{r}_g(i,j)$  may be assessed from a time-series of Meteosat observations converted into radiances  $L^t(i,j)$ . The analysis of several years of images from Meteosat shows that it happens that some pixels exhibit very low radiances, similar to those observed during the night, while the sun is well above the horizon. A constraint is imposed on radiances to avoid such cases; they should be greater than 3 percent of the maximal radiance that can be observed by the sensor:

$$L^t(i,j) \geq 0,03 \frac{I_{0met}(t)}{p} + b(t)$$

where  $b(t)$  is the calibration coefficient, and more exactly the radiance measured when viewing darkness. The calibration coefficients are obtained through the web site (see online at <http://www.helioclim.org>).

Knowing the Linke turbidity factor and the site elevation (see on line at <http://soda.jrc.it>), the path radiance is computed:

$$L_{atm}^t(i,j) = \frac{D_c^t(i,j) I_{0met}}{2 p I_0 (\cos q_v)^{0.8}}$$

and

$$\mathbf{r}_{atm}^t(\mathbf{q}_s, \mathbf{q}_v, \mathbf{y}) = \frac{p L_{atm}^t(i,j)}{I_{0met} e \cos q_s}$$

Finally, we get a quantity  $\mathbf{r}^{*t}(i,j)$  that is a ground albedo if the sky were clear at the instant  $t$ .

$$\mathbf{r}^{*t}(i,j) = [\mathbf{r}^t(i,j) - \mathbf{r}_{atm}(\mathbf{q}_s, \mathbf{q}_v, \mathbf{y})] / T(\mathbf{q}_s) T(\mathbf{q}_v)$$

This operation is performed for several images. For each pixel, a time series of  $\mathbf{r}^{*t}(i,j)$  is obtained. To eliminate artefacts in assessing the ground albedo, the time series is restricted to the instants for which the sun zenithal angle  $\mathbf{q}_s$  is less than the maximum of  $50^\circ$  and  $(2 \mathbf{q}_s^{noon} / 3)$ , where  $\mathbf{q}_s^{noon}$  is the angle observed at noon, remembering that  $\mathbf{q}_s$  is less than  $75^\circ$  in any case. The second minimum of the series of retained reflectances is the ground albedo  $\mathbf{r}_g(i,j)$  for this period.

The period of the time-series should be the shortest as possible in order to take into account the rapid variations of the ground albedo, if any. Compared to the method Heliosat-I, wherein it is preferable to have one estimate of the ground albedo per slot, the accurate correction of the effects of the sun and satellite angles permits to merge all the slots into the time-series. Thus, the period may be shortened. In an operational mode, especially when real time is at stake, a moving period may be adopted.

This possibility to have only one albedo map for a period permits to create a background map that allows overcoming the case where at a pixel, no cloudless instant is observed. In that case, the smallest reflectance is that of a cloud and should not be considered as the ground albedo. Prior being declared a ground albedo, the second minimum is compared to the background value. It cannot be less to half this value and cannot be greater than twice this value. If it is the case, it is set to one of these limits. The result is the ground albedo.

In our specific case, the background map was created by processing all images available for the months of January and December for the years 1985 to 1997. These months were selected as offering less questionable pixels for the whole field of view of the Meteosat satellite. For each pixel, the time-series of reflectances is processed as mentioned above. If less than 0.05 and if the pixel is over the land, the second minimum is set to this value. This background map was carefully screened by two operators to detect possible defects, using vegetation atlases and other geographical information.

## Annex F. The computation of the cloud albedo

The albedo of the clouds  $r_{cloud}$  has been defined by Cano (1982) as the typical value for the brightest clouds. The histogram of cloud albedoes is flat and it is very difficult to characterise this parameter  $r_{cloud}$  by a statistical quantity, such as a mode or a percentile. Costanzo (1994) or Hammer *et al.* (1997a, b) compute the mean value of the brightest albedoes observed in a time-series of images. The results may depend upon the length of the time-series and of the selected threshold. It should be added that some sites exhibit clear skies during several months (e.g. the Mediterranean basin), making it difficult to find very bright clouds.

The above-mentioned difficulties disappear if one is using calibrated radiances. In this case, we may adopt an actual albedo of the brightest clouds. Rigollier (2000) refers to the maximum value given by Grüter *et al.* (1986), that is 0.9. According to the experience of L. Wald, who set up several implementations of the Heliosat-I method for various cases, as well as to the works of Möser, Raschke (1983), Grüter *et al.* (1986), Moussu *et al.* (1989), Stuhlmann *et al.* (1990), Raschke *et al.* (1991) and Wald (1998), this parameter is not a maximum value and should not be taken too high. The effective cloud albedo depends upon the sun zenithal angle. We follow the model proposed by Taylor, Stowe (1984a):

$$r_{eff}(i,j) = 0.78 - 0.13 [1 - \exp(-4 \cos(q_s)^5)]$$

However, the parameter  $r_{cloud}$  is to be compared to the quantities  $r^{*t}(i,j)$  that derive from the observed radiances to compute the cloud index  $n$ . For  $r^{*t}(i,j) = r^t_{cloud}(i,j)$ , the cloud index  $n$  should be equal to unity. It follows that the same equation should apply to the effective cloud albedo, leading to the apparent cloud albedo  $r^t_{cloud}(i,j)$ :

$$r^t_{cloud}(i,j) = [r_{eff}(i,j) - r_{atm}(q_s, q_v, y)] / T(q_s) T(q_v)$$

Two constraints are added, gained from experience:

$$r^t_{cloud}(i,j) > 0.2, \text{ otherwise } r^t_{cloud}(i,j) = 0.2$$

$$\text{and } r^t_{cloud}(i,j) < 2.24 r_{eff}(i,j), \text{ otherwise } r^t_{cloud}(i,j) = 2.24 r_{eff}(i,j)$$

The value 2.24 is the largest anisotropy factor observed by Taylor, Stowe (1984b) for the present geometrical configuration sun-pixel-sensor and thick water cloud.

### Annex G. The relationship between the cloud index and the global hourly irradiation

The clear-sky index  $K_{ch}$  is equal to the ratio of the hourly global irradiation at ground on a horizontal surface  $G_h$  to the same quantity but for clear skies  $G_{ch}$ :

$$K_{ch} = G_h / G_{ch}$$

The relationship between the cloud index and the clear-sky index is the following:

$$n^t < -0.2 \quad K_{ch} = 1.2$$

$$-0.2 < n^t < 0.8 \quad K_{ch} = 1 - n$$

$$0.8 < n^t < 1.1 \quad K_{ch} = 2.0667 - 3.6667 n^t + 1.6667(n^t)^2$$

$$n^t > 1.1 \quad K_{ch} = 0.05$$

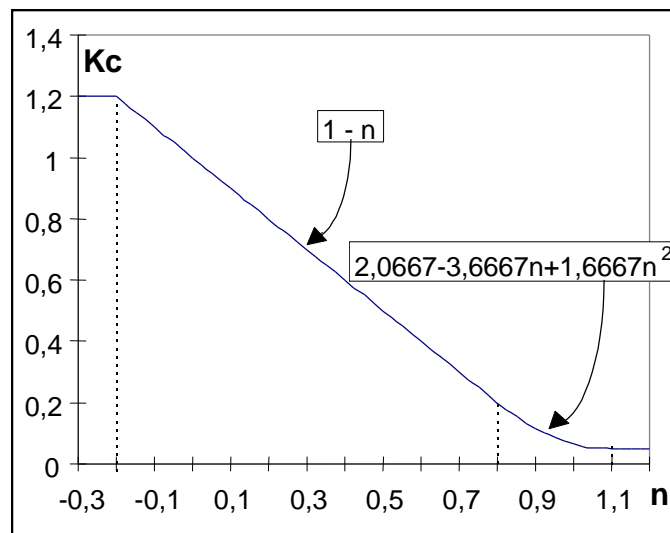


Figure 2. Relationship between the clear-sky index  $K_{ch}$  and the cloud index  $n$

## Annex H. The computation of the daily irradiation and subsequent quantities

The computation of the daily irradiation  $G_d(i,j)$  is based upon the  $N$  assessments of the hourly irradiation  $G_h(i,j)$  made during the day. The equations are the followings:

$$G_d(i,j) = K_{cd}(i,j) G_{cd}(i,j) = G_{cd}(i,j) \sum_{h=1}^N w_h K_{ch}(i,j)$$

$$\text{where } w_h = \frac{G_{ch}(i,j)}{\sum_{h=1}^N G_{ch}(i,j)}$$

It comes

$$G_d(i,j) = G_{cd}(i,j) \frac{\sum_{h=1}^N G_h(i,j)}{\sum_{h=1}^N G_{ch}(i,j)}$$

The estimate is said valid if at least  $N$  hourly irradiations are used in the computation. For each hourly irradiation, the mean solar elevation should be greater than  $15^\circ$ . To account for seasonal variation,  $N$  is set equal to a function of the sun zenithal angle observed at noon,  $q_s^{noon}$ .

*if  $q_s^{noon} < 55^\circ$ ,  $N = 2$ ; otherwise  $N = 3$  for the B2 data (data available every 3 hours)*

*if  $q_s^{noon} < 55^\circ$ ,  $N = 5$ ; otherwise  $N = 8$  when hourly values are available*

Other quantities are subsequently computed: the cumulative of the daily irradiation during 5 days or 10 days and the monthly mean of the daily irradiation.

These quantities are said valid if they are computed with at least 60 % of valid daily irradiation. It means that

- 5-days irradiations are made from at least 3 daily estimates (60 %),
- 10-days irradiations are made from at least 6 daily estimates (60 %),
- monthly means of daily irradiation are made from at least 18 daily estimates (60 %).

## Annex I. Solving the specific case of sun glitter on the ocean

The pattern of dancing highlights caused by the reflection of the sun from a water surface is called the sun glitter pattern. The surface of the ocean may be differentiated into small, mirrorlike facets. At spacecraft altitude, the reflecting facets will not be individually resolved. Therefore the apparent radiance of the sea surface in any direction will depend on the fraction of the area having the proper slope for specular reflection. The observed glitter pattern shows a radiance decreasing smoothly outward from its centre, since greater and therefore less frequent slopes are required as the distance from the centre increases. As the surface roughness increases with sea state, the pattern broadens and the level of radiance at the centre decreases (Wald, Monget 1983a).

Contrary to the usual case of ground reflectance, the reflectance of the sea is highly variable during a day, ranging from null values to values greater than cloud reflectances (Wald, Monget 1983b). The approach adopted to assess the ground albedo is not effective in the case of the glitter pattern. The glitter pattern is centred on the specular point that is approximately defined as the pixel for which the viewing and sun zenithal angles are equal and the difference of the azimuths of the sun and the satellite is equal to  $180^\circ$  (they are opposite). Far from the specular point, the ocean reflectance is approximately constant and the ground albedo approach is suitable.

Figure 3 exhibits the image acquired in the visible band by the Meteosat satellite. Visible in the middle of the image is the glitter pattern, a circle like shape in this case. The sun is at its zenith; the specular point is roughly southward of the nadir of the satellite.

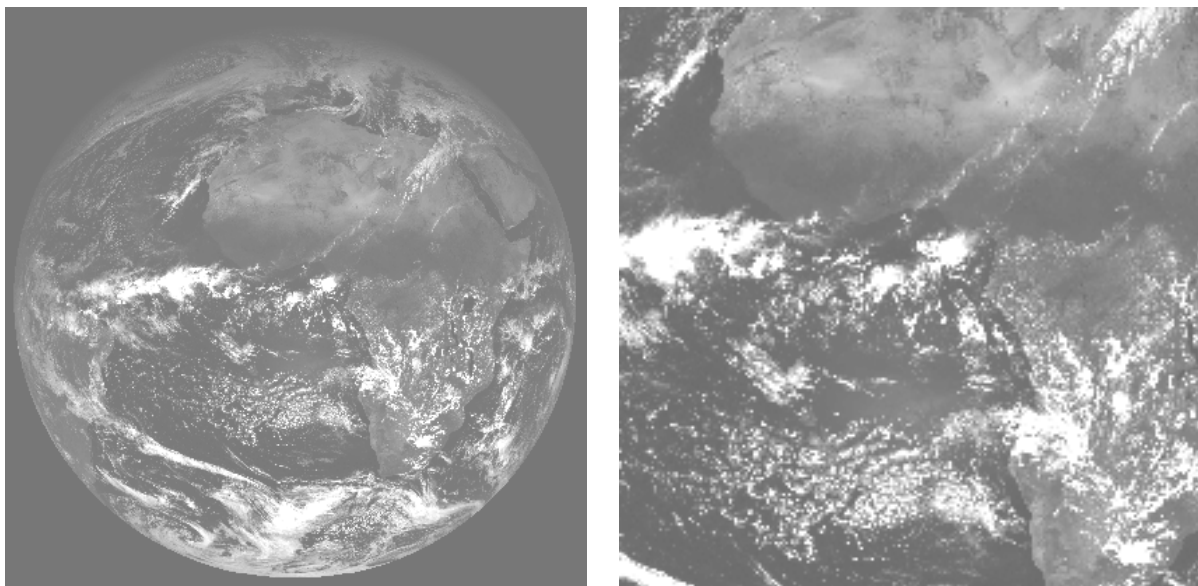


Figure 3. Meteosat visible image, taken on 1/1/1994, slot 23. Reflectances increase from black to white. The satellite is located above the Gulf of Guinea. Note the circular clear pattern in this Gulf, at the centre of the image, partly covered by clouds. The Gulf is magnified on the right image.

Within the glitter pattern, another approach should be designed to take into account the fact that the reflectance may be greater than that of a cloud. For practical reasons, it was decided to correct the cloud index in the glitter pattern instead of the reflectance.

A window is defined centred on the specular point. This point is defined as the pixel of the image for which the viewing and sun zenithal angles are the closest and the difference of the azimuths of the sun

and the satellite is the closest to  $180^\circ$ . The search is performed between the latitudes  $30^\circ\text{N}$  and  $-30^\circ\text{S}$  approximately. The viewing and zenithal angles should be greater than  $40^\circ$ . Otherwise, no correction is applied. The window is large enough to encompass the largest size of the glitter pattern: approximately 2000 km in radius. Only are considered the pixels known as belonging to the ocean. For each of these pixels, if the cloud index is greater than 0.2 ( $K_{ch}$  less than 0.8), the sky is said cloudy and no correction is applied. Otherwise, a new window of  $3 \times 3$  pixels is defined centred on the current pixel. One counts the number of pixels exhibiting cloud indices less than 0.2. If this number is strictly greater than 5 (60 % of the total), the current pixel is considered as cloud-free and the cloud index is set to 0.

Figure 4 shows the application of the method on the previous image (Fig. 3). The uncorrected map exhibits cloud indices that are too high in the glitter pattern. They are mistaken as clouds and the resulting irradiation will be too low. Once corrected, the cloud indices offer values that are similar to the other cloudless parts of the ocean. The clouds are not affected by the corrections.

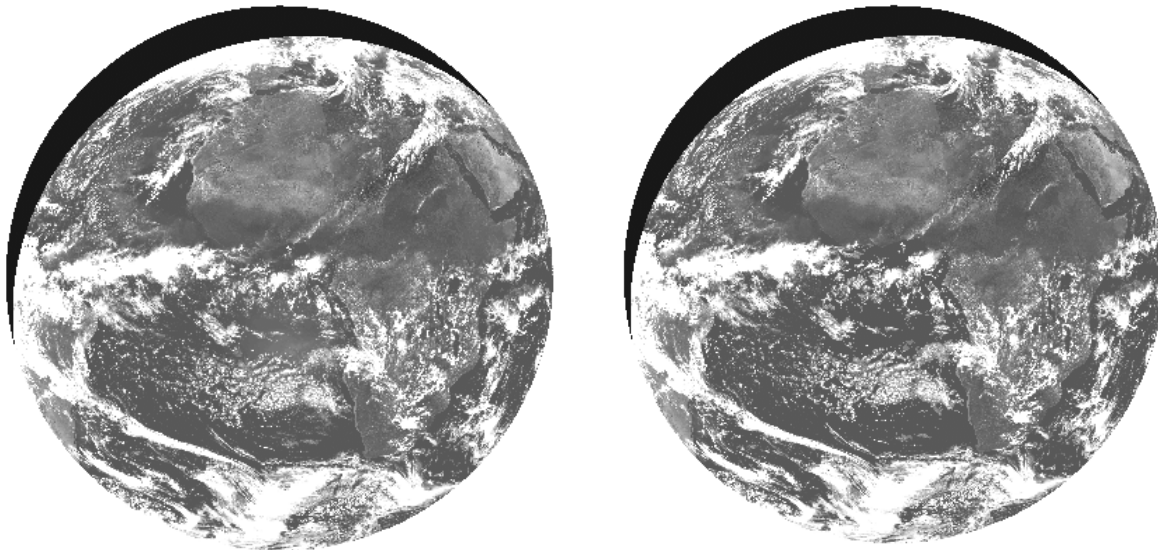


Figure 4. Map of the cloud index. Left: not corrected for the glitter effects. Note that the glitter pattern is clearly visible. Right: corrected.

## Annex J. An additional correction to hourly irradiation estimates

Detailed analyses of the discrepancies between ground measurements and Heliosat-II estimates revealed a bias that is a function of the true solar time. The exact reasons are unknown. They are believed to be a consequence of the approximate modelling of the influence of the solar zenithal angle in the joint assessment of the ground albedo, cloud albedo and instantaneous albedo.

The influence is not large at all and amounts to approximately 1-2 % in relative value. However, correcting for bias is very important in climate studies. An additional correction is brought to the clear-sky index,  $K_{ch}$ , computed in Annex G:

$$new K_{ch} = K_{ch} - 0.01(8 TST - 104)$$

where  $TST$  is the true solar time, and

$$new K_{ch} = \max(new K_{ch}, 0.05)$$

$$new K_{ch} = \min(new K_{ch}, 1.2)$$